SITE SPECIFIC DESIGN OPTIMIZATION OF A HORIZONTAL AXIS WIND TURBINE BASED ON MINIMUM COST OF ENERGY

A THESIS SUBMITTED TO
THE GRADUATE SCHOOL OF NATURAL AND APPLIED SCIENCES
OF
MIDDLE EAST TECHNICAL UNIVERSITY

BY

ECE SAĞOL

IN PARTIAL FULFILLMENT OF THE REQUIREMENTS
FOR
THE DEGREE OF MASTER OF SCIENCE
IN
AEROSPACE ENGINEERING

JANUARY 2010

Approval of the thesis:

SITE SPECIFIC DESIGN OPTIMIZATION OF A HORIZONTAL AXIS WIND TURBINE BASED ON MINIMUM COST OF ENERGY

submitted by **ECE SAĞOL**¸ in partial fulfillment of the requirements for the degree of **Master of Science in Aerospace Engineering Department, Middle East Technical University** by,

Prof. Dr. Canan Özgen ________
Dean, Graduate School of **Natural and Applied Sciences**

Prof. Dr.Ozan Tekinalp ________
Head of Department, **Aerospace Engineering**

Asst. Prof. Dr. Oğuz Uzol ________
Supervisor, **Aerospace Engineering Dept., METU**

Asst.Prof. Dr. Nilay Sezer Uzol ________
Co-Supervisor, **Mechanical Engineering Dept., TOBB ETU**

Examining Committee Members:
Prof. Dr. Serkan Özgen ____________________
Aerospace Engineering Dept., METU

Asst. Prof. Dr. Oğuz Uzol ____________________
Aerospace Engineering Dept., METU

Asst. Prof. Dr. Demirkan Çöker ____________________
Aerospace Engineering Dept., METU

Asst. Prof. Dr. D. Funda Kurtuluş ____________________
Aerospace Engineering Dept., METU

Prof. Dr. Ünver Kaynak ____________________
Mechanical Engineering Dept., TOBB ETU

Date:____________________

I hereby declare that all information in this document has been obtained and presented in accordance with academic rules and ethical conduct. I also declare that, as required by these rules and conduct, I have fully cited and referenced all material and results that are not original to this work.

Name, Last name: Ece SAĞOL

Signature :

ABSTRACT

SITE SPECIFIC DESIGN OPTIMIZATION OF A HORIZONTAL AXIS WIND TURBINE BASED ON MINIMUM COST OF ENERGY

Sağol, Ece

M.Sc., Department of Aerospace Engineering
Supervisor: Asst. Prof. Dr. Oğuz Uzol
Co-Supervisor: Asst. Prof. Dr Nilay Sezer Uzol

January 2010, 102 pages

This thesis introduces a design optimization methodology that is based on minimizing the Cost of Energy (COE) of a Horizontal Axis Wind Turbine (HAWT) that is to be operated at a specific wind site. In the design methodology for the calculation of the Cost of Energy, the Annual Energy Production (AEP) model to calculate the total energy generated by a unit wind turbine throughout a year and the total cost of that turbine are used. The AEP is calculated using the Blade Element Momentum (BEM) theory for wind turbine power and the Weibull distribution for the wind speed characteristics of selected wind sites. For the blade profile sections, either the S809 airfoil profile for all spanwise locations is used or NREL S-series airfoil families, which have different airfoil profiles for different spanwise sections, are used,. Lift and drag coefficients of these airfoils are obtained by performing computational fluid dynamics analyses. In sample design optimization studies, three different wind sites that have different wind speed characteristics are selected. Three scenarios are generated to present the effect of the airfoil shape as well as the turbine power. For each scenario, design optimizations of the reference wind turbines for the selected wind sites are performed the Cost of Energy and Annual Energy Production values are compared.

Key-words: Horizontal Axis Wind Turbine, Wind Turbine Airfoil, Design Optimization, Cost of Energy, Annual Energy Production, Cost of Wind Turbine.

ÖZ

YATAY EKSENLİ BİR RÜZGAR TÜRBİNİNİN EN AZ ENERJİ MALİYETİNE DAYALI SİTEYE ÖZGÜ TASARIM OPTİMİZASYONU

Sağol, Ece
Yüksek Lisans, Havacılık ve Uzay Mühendisliği Bölümü
Tez Yöneticisi : Yrd. Doç. Dr. Oğuz Uzol
Ortak Tez Yöneticisi: Yrd. Doç. Dr Nilay Sezer Uzol

Ocak 2010, 102 Sayfa

Bu tezde belirli bir rüzgar sitesine özgü yatay eksenli bir rüzgar türbini için enerji maliyetini en aza indirmeye dayalı tasarım optimizasyon metodu sunulmuştur. Bu tasarım metodunda enerji maliyetinin hesaplanmasında, bir rüzgar türbini ile bir yılda üretilen toplam enerji miktarını hesaplayan Yıllık Enerji Üretimi modeli ve toplam rüzgar türbini maliyetinin yıllık yansımasını hesaplayan Kullanım Süresi Maliyeti modeli kullanılmıştır. Yıllık Enerji üretimi rüzgar türbinin gücü için Pal Elemanı-Momentum teorisi ve seçilen sitelere özgü rüzgar karakteristikleri için Weibull dağılımı kullanılarak hesaplanır. Pal Elemanı-Momentum analizi literatürdeki deneysel data kullanılarak doğrulanmıştır. Pala profil kesitleri için, ya tüm pala kesitlerinde S809 kanat kesiti profili kullanılmış ya da farklı pala kesitlerinde farklı profiller olacak şekilde NREL S-serisi kanat kesiti ailesi kullanılmıştır. Bu kanat profillerinin kaldırma ve sürükleme kuvveti katsayıları hesaplamalı akışkanlar dinamiği analizleri yapılarak hesaplanmıştır. Örnek tasarım optimizasyon çalışmaları için farklı rüzgar hızı özelliklerine sahip olan üç farklı rüzgar sitesi belirlenmiştir. Bu farklı siteler için referans rüzgar türbinleri oluşturulmuştur. Kullanılan kanat kesitlerinin ve türbin gücünün, enerji maliyetine etkisini göstermek için üç farklı tasarım optimizasyonu senaryosu oluşturulmuştur. Her senaryo için, referans rüzgar türbinlerinin tasarım optimizasyonu belirlenen rüzgar sitelerine göre yapılmış ve enerji maliyetleri ve Yıllık Enerji üretim miktarları karşılaştırılmıştır.

Anahtar Kelimeler: Yatay Eksenli Rüzgar Türbini, Rüzgar Türbini kanat profili, Tasarım Optimizasyonu, Enerji Maliyeti, Yıllık Enerji Üretimi, Rüzgar Türbini Maliyeti

ACKNOWLEDGEMENTS

First of all, I would like to give special thanks to my advisor, Asst. Prof. Dr. Oğuz Uzol. Through his guidance, I have gained invaluable experience and insight related to not only in wind energy but also in propulsion. I could not have had a better advisor.

I would also like to thank to my co-advisor Asst. Prof. Dr. Nilay Sezer Uzol for her help and supports.

Thanks to Asst. Prof. Dr. İlkay Yavrucuk for allowing me to use the Neural Networks code written by him.

Finally I want to thank the many people who helped me with this study. They know who they are.

TABLE OF CONTENTS

LIST OF TABLES

TABLES

LIST OF FIGURES

FIGURES

LIST OF SYMBOLS

AEP	Annual Energy Production (MWh)
c	Weibull Scale Parameter (m/s)
c_{root}	Root chord (m)
c_{mid}	Mid-radius chord (m)
c_{tip}	Tip-radius chord (m)
C_l, C_d	Lift and Drag Coefficients of the airfoil
COE	Cost of Energy (cents/kWh)
D	Diameter of the rotor (m)
k	Weibull Shape Parameter
n	Number of the blade
r_{tip}	Tip radius (m)
r_{mid}	Mid radius (m)
r_{root}	Root radius (m)
r_{hub}	Hub radius (m)
Q	Tip loss factor
U	Wind Speed (m/s)
μ	Availability of the Wind Turbine
$\emptyset_{root}$	Root-radius Twist angle (^{o})
$\emptyset_{mid}$	Mid-radius Twist angle (^{o})
$\emptyset_{tip}$	Tip radius Twist angle (^{o})
θ	Inflow angle (^{o})
ω	Rotor speed (rpm)

CHAPTER 1

INTRODUCTION

Although there are numerous factors that drive the use of wind energy throughout the world, three among them dominantly impose the utilization of wind energy. First factor is the limited amount of fossil fuel resources. Energy demand has increased tremendously proportional to the population growth and technological developments. Although fossil fuels are the main energy resource, they are neither capable of meeting all energy requirement nor they are distributed evenly throughout the world. Due to these reasons, fossil fuel prices frequently become unstable generating many oil crisis situations. As a result, countries have been seeking for alternative energy resources that are both easily accessible and sustainable.

Another factor for the increased trend in the utilization of wind energy is the danger of global warming caused by the increased amount of greenhouse gases in the atmosphere due to the burning of fossil fuels. Kyoto Protocol [1], which targets to reduce the harmful gases in the atmosphere, has been accepted by many countries today. Reduction of atmospheric pollution can be achieved by utilization of green energy resources such as solar, wind and hydrodynamic energy.

Final factor is the need for potentially available and cheap energy resources. Wind energy is a favorable resource since it is available commonly and it is free. All these three factors bring out the wind energy as an alternative resource to fossil fuels in terms of being cheap, clean and potentially available.

Figure 1.1 shows that, the utilization of wind energy has been continuously increasing throughout the world. As can be seen, installed wind capacity was only 1743 MW in 1990, whereas it increased up to 40000 MW in 2003. Figure 1.1

also shows that, the increase in wind energy utilization mostly comes from the European Union countries.

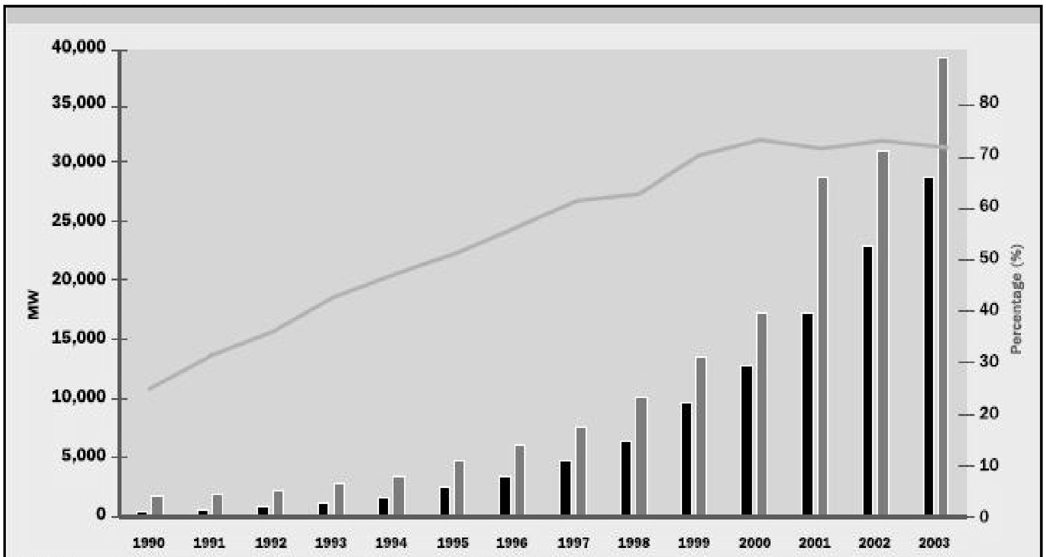

	1990	1991	1992	1993	1994	1995	1996	1997	1998	1999	2000	2001	2002	2003
EU-15	439	629	844	1,211	1,683	2,497	3,476	4,753	6,453	9,678	12,887	17,315	23,098	28,440
WORLD	1,743	1,983	2,321	2,801	3,531	4,821	6,104	7,636	10,153	13,594	17,357	28,857	31,128	39,500
EU % of world	25	32	36	43	48	52	57	62	64	71	74	73	74	72

Figure 1.1 Annually Installed Wind Capacity through world and EU-15 countries [2]

Market share distributions show that Germany holds the dominant amount of the wind energy production throughout the world as shown in Figure 1.2.

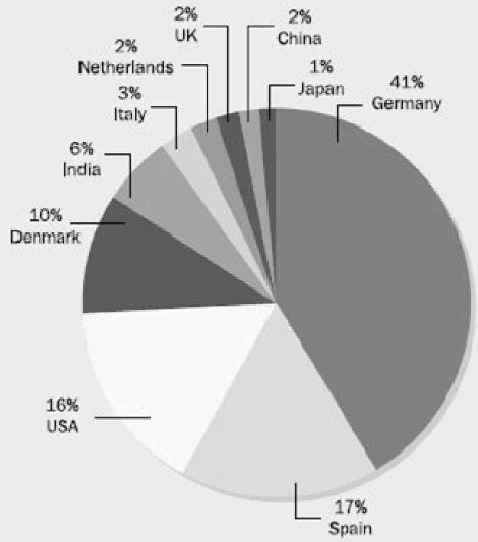

Country	Cumulative Installed Capacity End, 2002	% Share
Germany	12,001	41.4
Spain	4,830	16.7
USA	4,685	16.2
Denmark	2,880	9.9
India	1,702	5.9
Italy	785	2.7
Netherlands	688	2.4
UK	552	1.9
China	468	1.6
Japan	415	1.4
Total	**29,006**	**100.0**

Figure 1.2 Top 10 countries sharing Wind Energy Market in 2002 (MW) [2]

1.1 Historical Development of the Wind Turbine

Wind energy has been utilized for about 3000 years, starting with the invention of windmills, which are machines that convert wind energy to mechanical energy for milling and water pumping purposes. First examples of vertical axis windmills are found in China and Afghan-Persian regions [3]. The first horizontal axis windmills were invented in Europe and they were developed, especially in Holland region. An example of an advanced Dutch type windmill can be seen in Figure 1.3.

Figure 1.3 Windmill (Dutch ground windmill) with spring sails [3]

There are important milestones in the evolution of windmills from simple mechanical power producing machines to modern electricity producing wind turbines. First step was the attempt to modify windmills to generate electricity, which was achieved by Poul La Cour [3], a Danish professor. Industrialization of successful trials of first “wind turbines” was accelerated due to increased price of oil during World War I and they were used for electrification of rural areas even after World War II [3]. Another milestone, achieved by the German scientist Albert Betz in 1920, was the theoretical proof that the maximum possible potential energy in the wind is limited. Moreover, his works on aerodynamic shaping of rotor blades are important sources of development for modern wind turbines. Although many experimental wind turbines are constructed and tested in different sizes, they could not be industrialized since their prices were not low enough to compete with the very low fossil fuel prices. So a successful attempt could not be achieved until the “Energy Crisis” in 1973.

Development of modern wind turbines accelerated after the establishment of various scientific institutions on wind energy in different countries to reduce the dependence on the fossil fuels [3].

Today, three bladed, upwind wind turbines dominate the market for grid connected applications. Three bladed configurations are popular mainly due to easy handling of rotor moment inertia and aesthetic aspects [4]. Moreover since it is not an efficient way to use wind turbines as isolated units, wind farms are constructed to maximize the power production from a selected wind site.

1.2 Wind Turbine Components

Components of a typical modern Horizontal Axis Wind Turbine (HAWT) are shown in Figure 1.4. Electricity is generated by the rotational motion of the aerodynamically shaped rotor blades. Blade pitch mechanism and yaw system together help to extract maximum possible energy by controlling the angle of attack to the rotor blades and the direction of the rotor, respectively. Gearbox, rotor brake, generator and control system are part of the drive train, whose function is to convert mechanical energy to electricity. Whole system is supported by the tower and the foundation. Since large scale wind turbines are usually connected to national electrical networks (grid), the transformer unit balances the frequency of the generated electricity by wind turbine to the grid frequency.

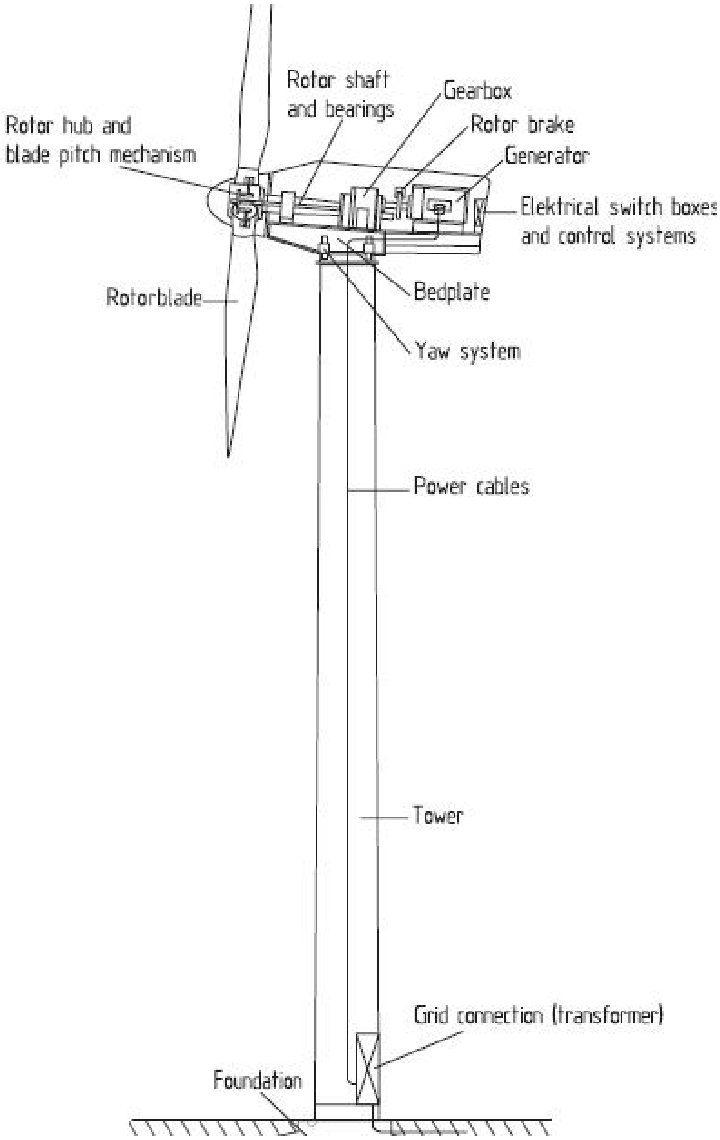

Figure 1.4 Components of a HAWT [3]

1.3 Wind Turbine Design Literature Survey

Wind turbine design is mainly based on various disciplines such as aerodynamic, performance, reliability, environmental considerations, economical and site requirements. A typical design optimization procedure, based on these disciplines, is shown in Figure 1.5.

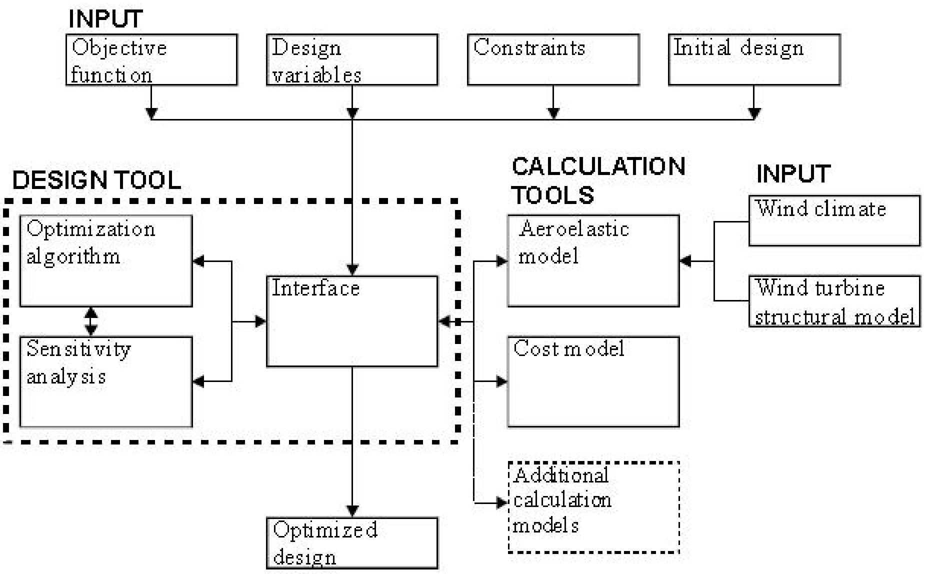

Figure 1.5 Wind Turbine Design Optimization Process [5]

Design of wind turbines were initially based on maximizing power at a single design operation point. As the design methods are aiming to sustain enhanced energy production capabilities with lower manufacturing and maintenance cost, new design concepts were developed. This motivation finally introduced the design methods based on lowest Cost of Energy (COE), which is the amount of expense for generating unit amount of energy. The Cost of Energy approach model the wind turbine through the whole wind speed regime instead of only near a single operating point. The COE model is explained in detail in [6]. Moreover, studies at wind energy laboratories such as National Renewable Energy Laboratory (NREL) [7], and at RISO [8] show the results of various design optimization studies based on Cost of Energy.

Basic model for cost calculation for wind turbines is given in [6], which is a function of the rotor diameter, the hub height, the rated power and the Annual Energy Production (AEP). A more involved model is presented in [8], which calculates the cost as a function of rotor loads. For the calculation of the amount of energy production, the Blade Element Momentum Theory is generally used in the literature as given in [9], [10] and [11].

Since different wind sites have different wind characteristics in general like the mean wind speed, frequency and direction, energy output of a wind turbine changes accordingly. Site specific design methods enable one to design wind turbines according to site wind characteristics so that maximum energy can be obtained throughout a year's period. In literature, there are a quite few number of papers on the investigation of site specific wind turbine design such as [5] and [8]

There also many studies in the literature on maximizing the performance of airfoils to increase the amount of energy production. NREL [12] and RISO [13] designed airfoils specific to wind turbine applications. In these studies type of the control system (i.e. pitch controlled or stall controlled), length of the blade and leading edge contamination of the blade are main design considerations.

1.4 Objectives and Content

This study introduces a design optimization methodology to obtain a three-bladed Horizontal Axis Wind Turbine (HAWT) that has the minimum "Cost of Energy" for a selected wind site with known wind speed characteristics. The Cost of Energy (COE) is basically defined as the annual cost of a wind turbine over the amount of annual energy generated. The Cost of Energy model is based on NREL Scaling and Cost Model [6] which also includes a model for the calculation of Life Cycle Cost (LCC) of a wind turbine. Annual Energy Production (AEP) is obtained by calculating the power generated by a wind turbine and by utilizing the frequency of the wind for each speed from cut-in to cut-out speeds of wind turbine. Power production is obtained using Blade Element Momentum (BEM) [9] method and wind speed frequency is modeled using Weibull probability density distributions. A Genetic Algorithm based optimization routine [14] has been implemented into the design procedure. The design optimization parameters are selected as the chord and the twist distributions as well as the rated power. The objective function for optimization is the minimum "Cost of Energy".

Three scenarios have been generated to evaluate the effect of different parameters on Cost of Energy. First and second scenarios try to find the optimum chord and twist distributions for a constant rated power. The first scenario uses a single airfoil profile that does not change through the blade span, and the second scenario uses NREL airfoil family that has a pre-determined airfoil variation across the span. Third scenario includes the rated power also as an optimization parameter along with the others. For each scenario, design optimization is performed for three different wind sites, whose Weibull parameters are known, to evaluate the effect of different wind characteristics on wind turbine performance and COE.

The presentation of this thesis is structured on five main parts, the design optimization methodology, Annual Energy Production Model, Life Cycle Cost Model, airfoil database generation and sample applications of the design optimization methodology

In Chapter 2, the details of the design optimization problem and methodology are given. The general outlines of the design tools, such as the Cost of Energy definition, Annual Energy Production and Life Cycle Cost models are introduced. The optimization algorithm, optimization parameters and constraints are given in this chapter.

Chapter 3 presents the Annual Energy Production model in detail. Theoretical background on the Blade Element Momentum Analysis, used for power production calculation, is given. Modeling of the wind speed frequency by Weibull analysis is also explained.

The details of the Life Cycle Cost model are presented in Chapter 4, which include all of the algebraic equations for the cost calculation of various wind turbine components.

Chapter 5 presents the aerodynamic characteristics of airfoils used in the design optimization. The details of the derivation of lift and drag coefficients by numerical methods in order to generate the database needed by the BEM are presented in this chapter.

Finally, the results of sample design optimization studies for selected wind sites are presented in Chapter 6. The Weibull distributions of selected wind sites are also given in this chapter.

CHAPTER 2

DESIGN OPTIMIZATION METHODOLOGY

2.1 Introduction

In modern engineering, Multidisciplinary Design Optimization (MDO) concept is generally used in designing complex systems. MDO enables evaluation of different disciplines that relates to the system, simultaneously. In wind turbine design aerodynamics, structures, reliability, performance, cost, controls and noise are the disciplines that are considered. Besides handling various disciplines, MDO takes the advantage of accomplishing the design and optimization process also simultaneously.

In this study, the design optimization is based on different disciplines such as the economy, aerodynamics and performance, using Cost of Energy (COE) model. Cost of Energy (COE) is defined as [6];

$$COE = \frac{FCR * ICC + AOE}{AEP} \tag{2.1}$$

Cost components are made of ICC, FCR and AOE. ICC is the Initial Capital Cost of the wind turbine in American dollars ($) that covers wind turbine costs and Balance of Station costs. FCR is the Fixed Charge Rate that is the annual rate of money that should be paid to cover ICC. FCR is dimensionless and depends on the amount of year that ICC is covered and taken as 0.1158 for 10 year period [6]. AOE is the Annual Operating Expenses in American dollars ($), which covers the fees that are paid annually as Operating & Maintenance and land rental fees.ICC and AOE are computed as a function of the rotor diameter, the hub height, the rated power and Annual Energy Production. Details of ICC and AOE cost models are given in Chapter 4 Life Cycle Cost Model.

The technological parameter, AEP is the Annual Energy Production in MWh and is a function of both the wind characteristics of a wind site as well as the engineering design parameters of a wind turbine. It is calculated through a wind analysis that is based on Weibull probability density distributions and a Blade Element Momentum (BEM) Analysis to compute the power generated at different wind speeds. A genetic algorithm based optimization routine is used for searching for the turbine that has the minimum COE for a specific wind site. Figure 2.1 summarizes the design optimization methodology.

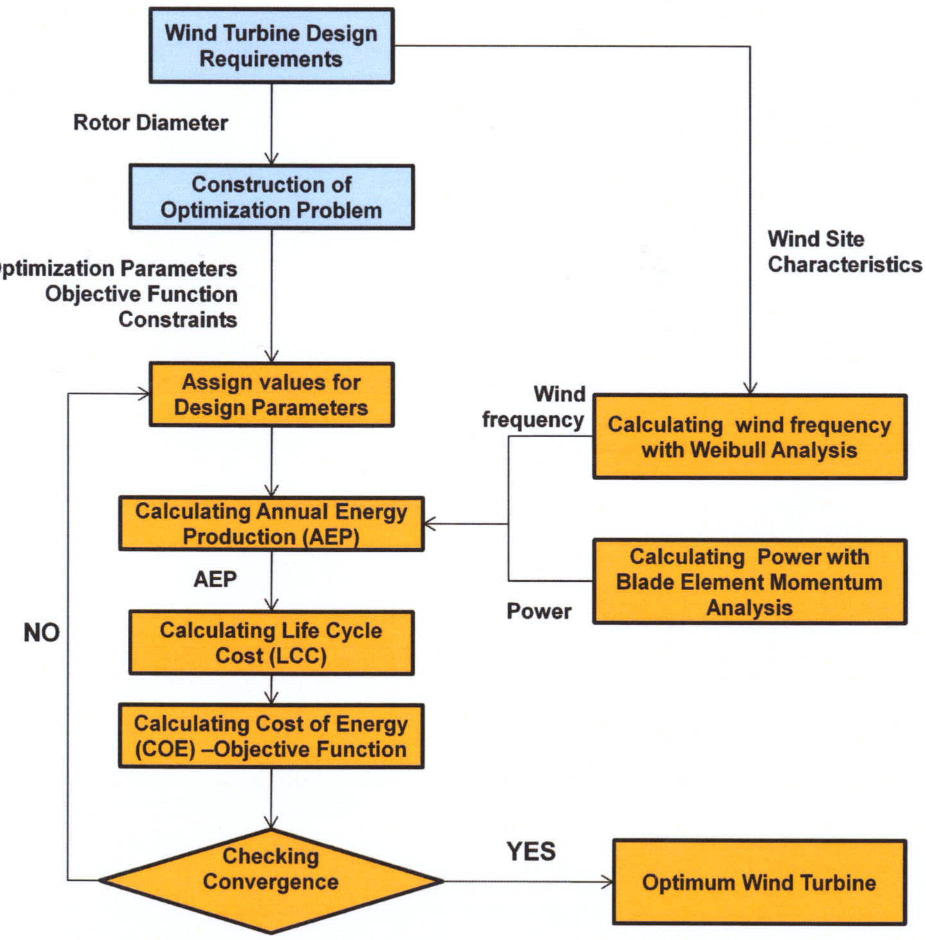

Figure 2.1 Multidisciplinary Design Optimization process algorithm

The very first step of the design optimization process is the determination of the fundamental design requirements and constraints such as the selection of the wind site and the diameter of the rotor. Based on energy requirements, customers and designers together decide the size of the wind turbine. In a similar way, the customers might indicate their preferences of wind sites since the wind turbine will be designed according to the site characteristics. After the selection of the wind sites, Weibull characteristics of selected sites should be obtained and made available.

After the design requirements are determined, the optimization problem is constructed by selecting an appropriate objective function, optimization parameters and constraints. The objective function for this study is selected as minimum Cost of Energy (COE), defined as the expense of generating unit amount of energy. The optimization parameters are chord and twist distributions along blade span as well as the rated power. The blade area is restricted during the optimization process to avoid unphysical chord and twist values.

The optimization process starts by assigning values to the design optimization parameters by optimization code. Using the assigned design parameters, initially, the Annual Energy Production (AEP) of each new design is calculated. The AEP, which is the total energy generated by a unit wind turbine in a year, is characterized by the power performance of the wind turbine and wind frequency at certain wind speeds. Power of the wind turbine is calculated using Blade Element Momentum Analysis which is a very popular method in calculating power of rotary systems such as helicopter rotors, propellers and wind turbines. Meanwhile, wind frequency is calculated using Weibull Analysis by defining a distribution function for speed over time. Wind Site characteristics, needed for Weibull Analysis, are predetermined at Wind Turbine Requirements section.

Following the AEP module, Life Cycle Cost (LCC) of wind turbine is calculated. LCC is defined as the amount of money that shall be paid in a year’s period. LCC covers all type of wind turbine costs as manufacturing, engineering, material, operation and maintenance, installation and many other costs.

Using AEP and LCC, Cost of Energy (COE) for each new design is calculated by dividing the LCC to AEP. In the design optimization algorithm, convergence of the design is checked. If design is agreed to be converged, optimum wind turbine is achieved. Otherwise optimization process is restarted.

An in-house code, WindCOE, is developed based on the design optimization algorithm explained above. As inputs, WindCOE needs mathematical definition of objective function, optimization parameters, wind site characteristics and fundamental wind turbine dimensions as rotor diameter and hub height. As a result of optimization, geometrical characteristics and rated power of the optimum wind turbine that gives the minimum COE for the selected wind site is obtained.

2.2 The Optimization Tool

In this section, the Genetic Algorithm optimization tool, and the details of the optimization problem are explained.

2.2.1 Genetic Algorithm

The objective of the optimization is to find the optimum combination of desired parameters to achieve a target performance. Genetic Algorithms (GA) are optimizers based on a global search of the design space by stochastic methods. Genetic Algorithms obey the genetics and natural selection principles of Darwin.

In natural selection process, individuals, having characteristics adapted to the environment, survive to generate new populations. On the contrary, individuals, having characteristics not adapted to the environment, fail to survive. Therefore new generations always have improved characteristics, in other words, population is optimized to be adaptive against environment. Genetic Algorithms, similar to the natural selection process, evaluate the population in terms of fitness with respect to an objective function.

In an optimization process, certain parameters need to be defined to construct an optimization problem. These are;

The Objective function: Targeted function to be maximized or minimized.

Optimization parameters: Parameters to be optimized to maximize or minimize objective function.

Constraints: Maximum and minimum boundaries of optimization parameters and other limitations to keep design in physical limits.

Genetic Algorithms have their own terminology in expressing the optimization parameters. These are;

Individual: Possible design solution.

Population: Design set composed of individuals

Chromosome: Optimization parameters of an individual expressed in binary system

Fitness: Best solution to the objective function.

Typical flowchart of the GA is given in Figure 2.2. Before the optimization process, the objective function, optimization parameters, constraints and GA parameters such as the mutation rate, the crossover rate, and the number of individuals in a population are determined. After the optimization problem is constructed, optimization process is started by the generation of an initial population through random selection of individuals in a binary system. These individuals are then converted to the decimal system to define the values of the each optimization parameter. Fitness of each individual is calculated using the objective function and individuals are sorted according to their fitness. In order to generate individuals for the next generation, these individuals are mated, in other words, their chromosomes are combined to generate new chromosomes. Besides, some of these individuals are mutated to maintain the diversity of the population. After the new population is generated, fitness of the individuals is calculated to check whether convergence is reached or not. Convergence of the optimization is controlled, by checking the best fitness of population. If the same fitness value repeats for a large number of iterations, the optimization process is agreed to reach a converged solution.

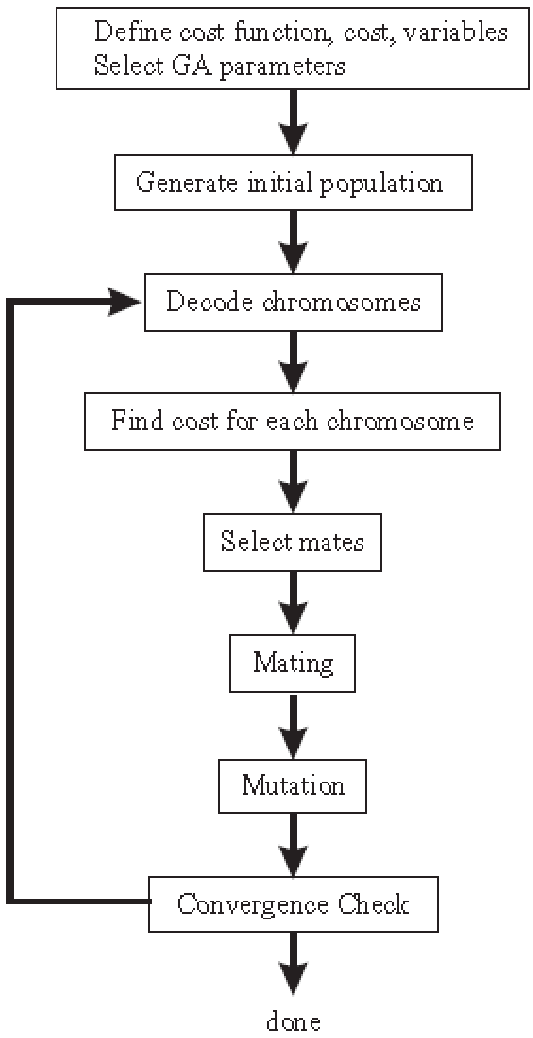

Figure 2.2 Flowchart of a classical Genetic Algorithm [15]

Genetic Algorithm is used in this study mainly due to its suitability to design problems. First of all Genetic Algorithms are easily implemented to the design codes. Moreover, they can deal with the large number of optimization parameters, which is the case in this study. Finally since they do not need derivatives of functions, they do not cause extra problems in terms of convergence.

2.2.2 Wind Turbine Optimization

Construction of the wind turbine optimization problem starts by defining the objective function, optimization parameters and optimization constraints.

Objective Function:

Maximum power output, minimum cost, minimum Cost of Energy, maximum Annual Energy Production are typical objective functions for wind turbine designs. In this study minimum COE is selected as the objective function.

Optimization Parameters:

As defined before, optimization parameters are the variables of the design that are used to generate new configurations. In wind turbine design, optimization parameters are usually twist and chord distributions, airfoil profiles, radius, tip speed, pitch angle, hub height and rated power. In this study, chord and twist distributions as well as the rated power are selected as optimization parameters.

- Chord Distribution:

  Chord distribution is defined as an optimization parameter and is represented by a second order polynomial that is defined by chord values at root, mid and tip sections of the blade. The second order polynomial is defined as;

$$A_1\, r^2 + B_1 r + C_1 = c(r) \tag{2.2}$$

  Unknown polynomial coefficients A_1, B_1 and C_1 are calculated using known c_{root}, c_{mid} and c_{tip} values for each design by solving the appropriate system of equations. Limits of the chord values are determined by considering limits of the similar size (diameter) commercial wind turbines [16].

- Twist Distribution:

  Similar to the chord distribution, twist distribution is also defined as an optimization parameter and represented by a second order polynomial through twist values at three locations on the blade as; $\emptyset_{root}, \emptyset_{mid}$ and $\emptyset_{tip}$. The second order polynomial is defined as ;

$$A_2\, r^2 + B_2 r + C_2 = \emptyset(r) \tag{2.3}$$

  Polynomial coefficients, A_2, B_2 and C_2 are determined using $\emptyset_{root}, \emptyset_{mid}$ and $\emptyset_{tip}$ values for each design by solving the appropriate system of equations. Limits of the twist values are determined by considering limits of commercial wind turbine [16].

- Rated Power:

  Rated power is the capability of the wind turbine to convert mechanical power to electrical power. It's generally restricted by the electrical generator selection. In this study, when the rated power is not selected as an optimization parameter, it is calculated using [2] ;

$$P_{rated} = 0.000195 D^{2.155} \tag{2.4}$$

All design optimization parameters are summarized in Figure 2.3

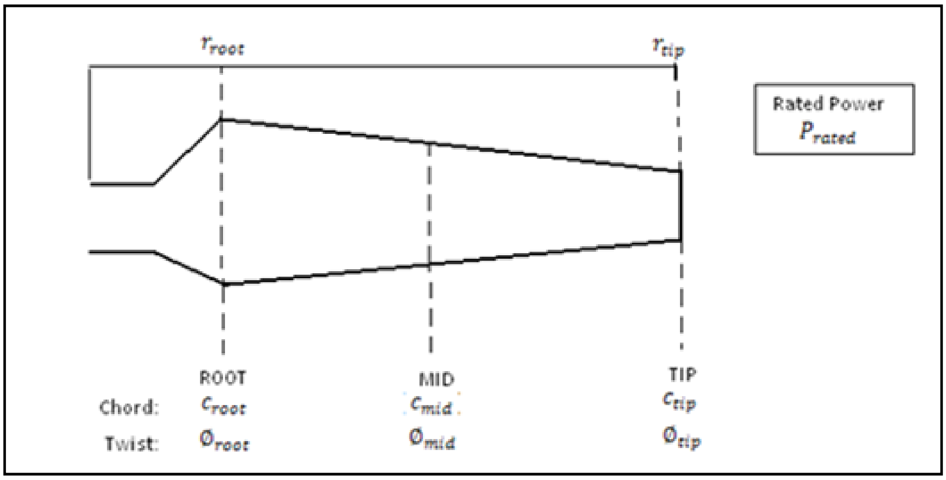

Figure 2.3 Representation of optimization parameters

Constraints:

Constraints are the limitations that prevent generation of unrealistic designs. Typical constraints used in wind turbines are physical limitations to blade size, noise level limits and load limits to prevent structural failure.

- Blade Area Constraint:

  In this study blade area is restricted by considering the limits of existing wind turbines [16]. Using different size commercial wind turbines, trendline for blade area is generated as shown in Figure 2.4. Restricting blade area both keeps blade size in physical limits and prevents formation of excessive blade loads. In WindCOE, blade area is limited according to rotor diameter of the design.

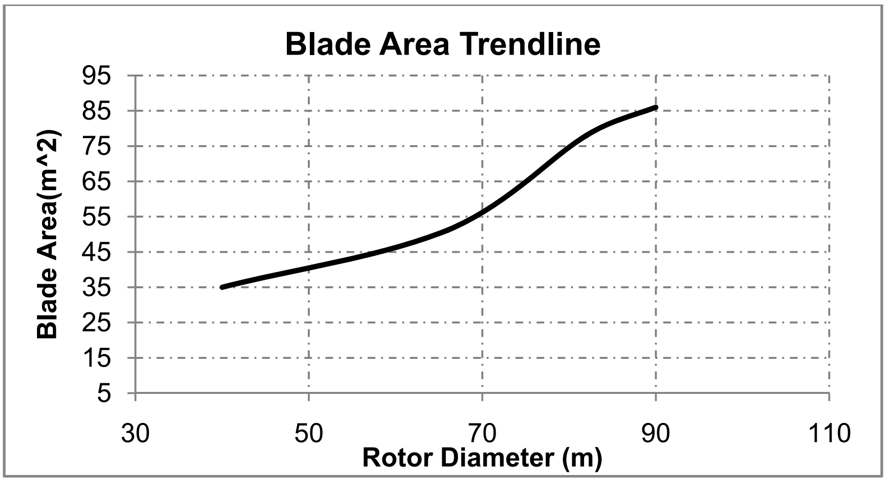

Figure 2.4 Trend line for wind turbine blade area

- Chord and Twist Constraints

Constraint for chord and twist are used for keeping the growth of these parameters in physical limits. In modern wind turbines, chord and twist decreases from root to tip, so following conditions are implemented on WindCOE.

$$c_{root} > c_{mid} > c_{tip} \tag{2.5}$$

$$\emptyset_{root} > \emptyset_{mid} > \emptyset_{tip} \tag{2.6}$$

Moreover, limits for optimization parameters are assigned to keep the optimized design in realistic size. For this purpose, chord and twist values of the existing designs are determined from [16]. Only wind turbines with rotor diameter larger than 40m is considered since the LCC model is applicable under this condition.

Trend lines of root and tip chord values are shown in Figure 2.5.a and b. Limits for the root and tip chords are assumed as 20% larger of trend line for upper limit and 20 % smaller of trend line for lower limit.

Since there is no data of mid-chord for commercial wind turbines, upper and lower limits for optimization are calculated as follows.

$$c_{mid,up} = \frac{c_{root,up} - c_{tip,up}}{2} \tag{2.7}$$

$$c_{mid,low} = \frac{c_{root,low} - c_{tip,low}}{2} \tag{2.8}$$

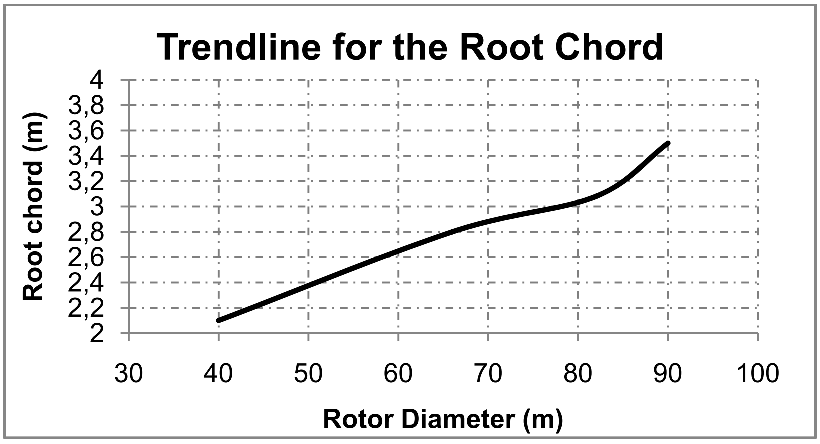

(a)

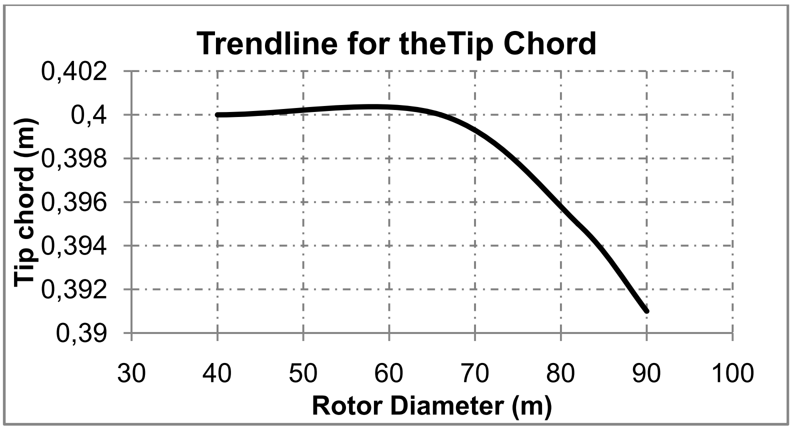

(b)

Figure 2.5 Trendlines for the root (a) and tip b) chord obtained from commercial wind turbines.

No trend line study is used for twist limits. Maximum and minimum twist values of existing wind turbines [16], are used as twist upper and lower limits in WindCOE. They are given in Results section for the sample design optimization study.

- Noise Constraint:

  The noise level is also kept within limits by restraining the tip speeds of the designs generated. Tip speed limit is taken from a trend study published by European Wind Energy Association (EWEA) [2] and used as 75 m/s. According to this reference, modern wind turbines with rated power higher than 1 MW have a noise level between 100 and 106 dB.

CHAPTER 3

ANNUAL ENERGY PRODUCTION MODEL

The Annual Energy Production (AEP) Model calculates the total energy generated by a specific wind turbine in a specific wind site, in a year period. The AEP calculation enables a designer to evaluate and compare the performance of different wind turbines operating at a specific wind site. The AEP is calculated using [6] ;

$$AEP = E_{gen} * \mu * Availability\ [kWh] \tag{3.1}$$

where μ is the efficiency of the wind turbine defined as,

$$\mu = (1 - SoilingLosses) * (1 - ArrayLosses) \tag{3.2}$$

Soiling losses are losses that cause reduction in total energy generated due to the accumulation of insects and dirt on the leading edge of the rotor blades. This deteriorates the shape of the airfoil profile resulting in a reduction in the lift coefficient. This parameter is taken as 3.5 % as suggested in [6]. In addition to the soiling losses, aerodynamic interference between wind turbines in a wind farm cause array losses, which is taken as 5 % in this study again as suggested in [6]. Availability, characterizes the degree of a wind turbine's operability in a year's period, and is taken as 98% as suggested in [6].

E_{gen} is the total energy that can be produced in a year and is defined as;

$$E_{gen} = \sum_{i=Vcut_{in}}^{Vcut_{out}} P(i) * Weibull(i) * \frac{8760}{4*1000}\ \ [kWh\} \tag{3.3}$$

Here, P(V_i) is the power output of the turbine at a specific wind speed V_i calculated through BEM analysis and Weibull (V_i) is the probability density function of the wind speed calculated using the Weibull parameters of a selected wind site. 8760 is the total number of hours in a year's period.

Blade Element Momentum Analysis and Weibull Analysis are explained in detail in the following sections.

3.1 Blade Element Momentum Analysis

The Blade Element Momentum (BEM) analysis is used for calculating the power produced at different wind speeds. This is a well-established two dimensional method that combines the Blade Element Theory and the Momentum Theory for rotors [17] and is widely used for power calculation especially in optimization studies due to its low computational cost. An in-house BEM code is developed for this purpose and used as a part of the WindCOE in this study. The code uses Prandtl Tip Loss Model [17] and the empirical relation developed by Buhl [18] to model the turbulent wake state that occurs at high tip speed ratios. Details are given in the following sections.

3.1.1 Momentum Theory

Momentum Theory is a one dimensional tool to investigate the flow using the principle of conservation of momentum. For rotating systems, conservation of momentum analysis is usually extended to both axial and tangential directions. Axial momentum analysis models the power of the wind turbine in terms of an axial induction factor, and the axial wind speed, whereas the rotational momentum analysis models in terms of a tangential induction factor and the rotational speed. For both analysis, flow is assumed to be steady, adiabatic and air is assumed as incompressible.

Axial Momentum Analysis

Momentum theory is one of the most fundamental approaches to wind turbine analysis and other rotary systems such as helicopters and propellers. It provides a rough estimation of the power output of a wind turbine, using basic inputs like the wind speed and the rotor disk area, by means of one dimensional analysis.

First assumption for this analysis is that the wind turbine rotor is treated as an actuator disk. Therefore the effects of individual blades are not taken into account. Moreover, since it is one dimensional no rotational effects are included. Figure 3.1 shows a typical control volume used in axial momentum analysis;

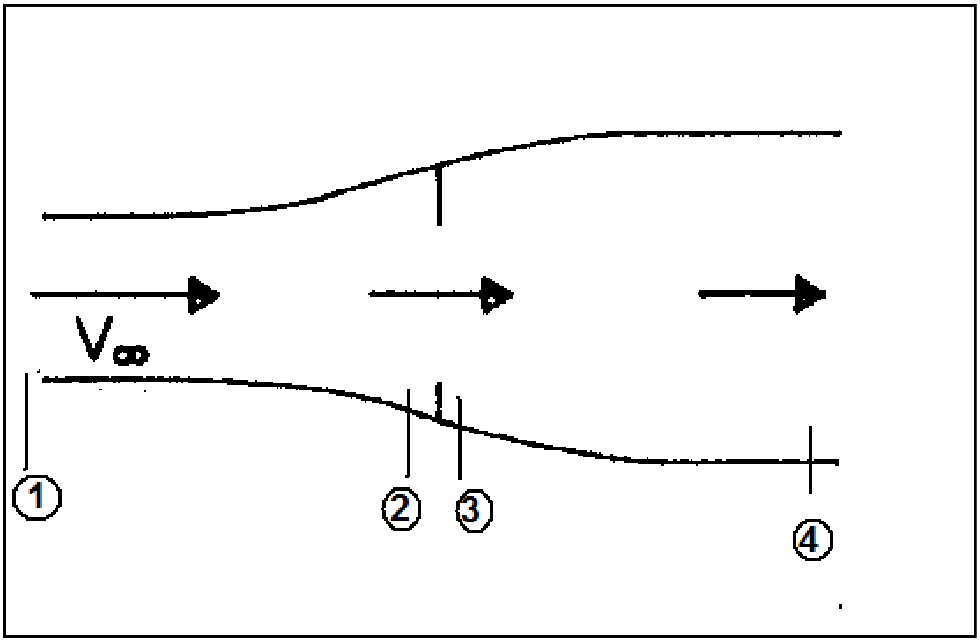

Figure 3.1 Control volume used in axial momentum analysis

No work is done both between station 1 and 2, and station 3 and 4. So, Bernoulli equation can be applied for these regions as;

$$p_1 + \frac{1}{2}\rho V_1^2 = p_2 + \frac{1}{2}\rho V_2^2 \tag{3.4}$$

$$p_3 + \frac{1}{2}\rho V_3^2 = p_4 + \frac{1}{2}\rho V_4^2 \tag{3.5}$$

Moreover, assuming pressure at station 1 and station 4 are freestream pressure and no velocity change between stations 2 and 3 as;

$$p_1 = p_4$$

$$V_2 = V_3$$

Using equations from 3.4 and 3.5 and assumptions above, pressure difference between station 2 and 3 is obtained as;

$$p_2 - p_3 = \frac{1}{2}\rho(V_1^2 - V_4^2) \tag{3.6}$$

Between stations 1 and 2, there is an axial induced velocity. This induced velocity is defined in non dimensional form as following.

$$a = \frac{V_1 - V_2}{V_1} \tag{3.7}$$

where a, is called axial induction factor. Therefore, V_2 and V_4 can be defined in terms of axial induction factora as;

$$V_2 = V_1(1 - a) \tag{3.8}$$

$$V_4 = V_1(1 - 2a) \tag{3.9}$$

Conservation of momentum through the differential disk area is defined as

$$(p_2 - p_3)dA = \rho(V_1 - V_4)dA\, V_2 \tag{3.10}$$

By replacing V_2 in conservation of momentum, resultant equation is;

$$(p_2 - p_3)dA = \rho(V_1 - V_4)V_1(1 - a)dA \tag{3.11}$$

Resultant power extracted between stations 2 and 3 are obtained using Equation 3.11 as;

$$dP = \frac{1}{2}\rho V_1^3(4a(1 - a)^2)2\pi r dr \tag{3.12}$$

Rotational Momentum Analysis

In the rotational momentum analysis, the rotational motion is given to the actuator disk by means of angular velocity, Ω.

Rotational motion exerts a torque on the system, and therefore the power can be calculated using the torque as;

$$dP = \Omega dQ \tag{3.13}$$

where the differential torque is defined as;

$$dQ = \rho V_2 \omega r^2 2\pi r dr \tag{3.14}$$

Here ω is the tangential induced velocity and the tangential induction factor a' is defined as;

$$a' = \frac{\omega}{2\Omega} \tag{3.15}$$

Substituting the tangential induction factor in to the differential force and torque equation, one can obtain,

$$dQ = 4a(1 - a')\rho V_1 \Omega r^3 \pi d\mathrm{r} \tag{3.16}$$

3.1.2 Blade Element Theory

The Blade Element Theory is used for aerodynamic performance prediction. In this analysis blade is divided into a number of sections as seen in Figure 3.2. Each two-dimensional airfoil section is evaluated independently in terms of lift and drag and then the force exerted by the rotor is calculated through the integration of these sections. Most important assumption for this analysis is that there is no interaction between blade sections. The velocity triangle on a blade element is shown in Figure 3.3.

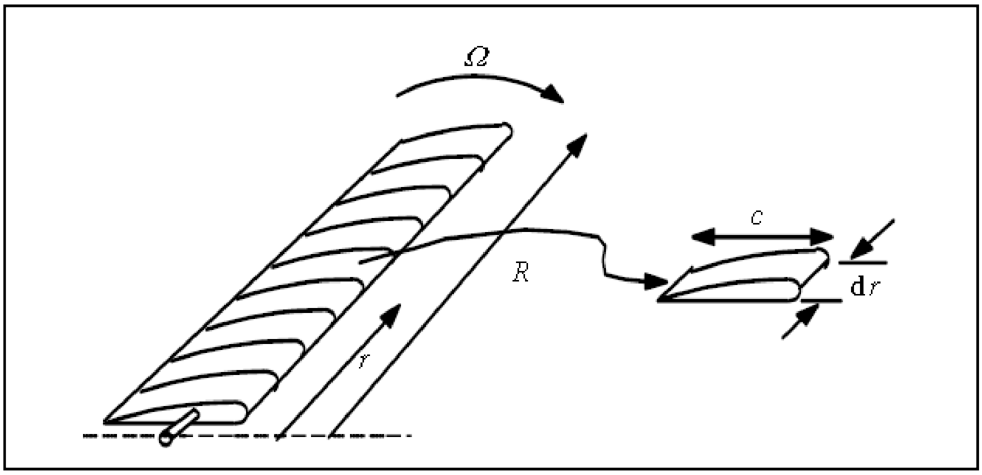

Figure 3. 2 Representation of the blade sections used in the Blade Element Analysis [19]

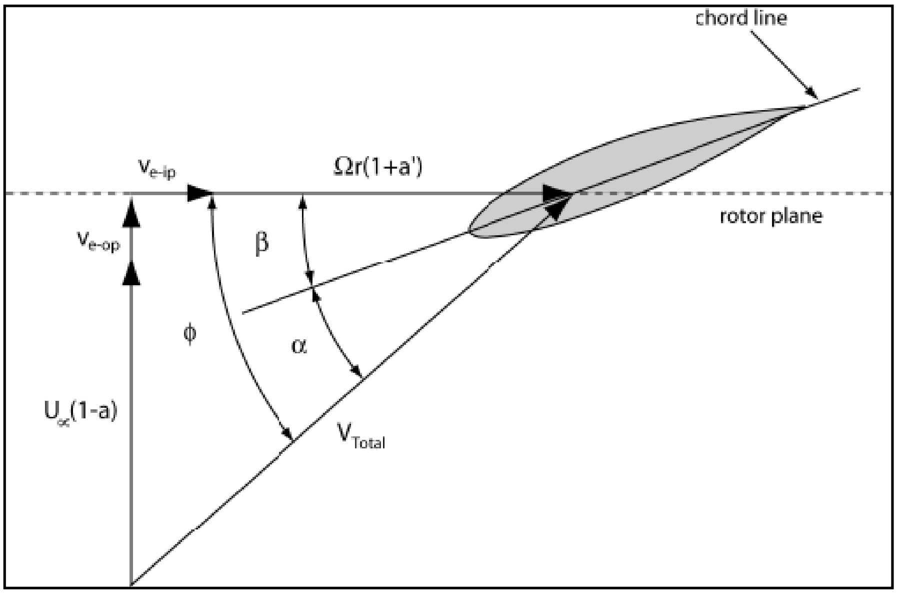

Figure 3.3 Wind turbine section angles [9]

The inflow angle, θ, is calculated from the velocity triangle as;

$$tan\theta = \frac{V_1(1-a)}{\Omega r(1+a')} \quad (3.17)$$

The angle of attack can be found by subtracting the geometric twist from the inflow angle as;

$$\alpha = \theta - \emptyset \tag{3.18}$$

Using the angle of attack, the lift coefficient,C_l and the drag coefficient, C_d can be obtained from numerical or experimental data.

Axial force and torque on blade elements are calculated as;

$$dF_x = N\frac{1}{2}\rho V_{tot}^2(C_l cos\theta + C_d sin\theta)cdr \tag{3.19}$$

$$dQ = N\frac{1}{2}\rho V_{tot}^2(C_l sin\theta - C_d cos\theta)crdr \tag{3.20}$$

where V_{tot} is;

$$V_{tot} = \sqrt{(\Omega r(1 + a'))^2 + (V_1(1 - a))^2} \tag{3.21}$$

3.1.3 Blade Element Momentum Theory

The Blade Element Momentum theory combines the momentum theory and blade element theory through force and torque equations. By equating force equation obtained from the axial momentum analysis, with that from the Blade Element Analysis, axial induction factor is obtained as;

$$a = [\frac{4Qsin^2\theta}{\sigma'(C_l cos\theta + C_d sin\theta)}]^{-1} \tag{3.22}$$

Equating the torque equations of the rotational momentum analysis and Blade Element Analysis, the tangential axial induction factor is obtained as;

$$a' = [\frac{4Qsin\theta cos\theta}{\sigma'(C_l sin\theta - C_d cos\theta}]^{-1} \tag{3.23}$$

Tip Loss Correction:

One deficiency of the two-dimensional BEM analysis is that the three dimensional effects like tip losses cannot be evaluated. Tip losses resulting from vortices shed from the tip regions, are modeled using the Prandtl Tip Loss Model, by means of an empirically developed correction factor as [17] ;

$$Q = \frac{2}{\pi} cos^{-1} \left[exp \left\{ -\frac{n}{2} \frac{R-r}{rsin\theta} \right\} \right] \tag{3.24}$$

Tip loss correction factor is directly implemented to the thrust and power equations as a multiplier. Equations 3.22 and 3.23 include Tip Loss Correction factor, Q.

<u>Glauert&Buhl Correction</u>

At high loading conditions, like start-up and shut-down, wind turbine enters a state called the turbulent wake state. For this state, momentum analysis is no longer valid, since it cannot predict the thrust coefficient correctly. The turbulent wake state exists when the axial induction factor is greater than 0.4. Glauert [17] developed a correction for this state to fit the thrust coefficient to experimental data, as shown below; Thrust coefficient with and without Glauert correction is shown in Figure 3.4.

$$C_T = 0.889 - \frac{0.0203 - (a - 0.143)^2}{0.6427} \tag{3.25}$$

Since the Glauert correction does not include the tip loss correction, it is only applicable when tip loss factor is assumed as 1. In order to include the tip loss effects, Buhl [18] developed an improved model based on Glauert's model as follows;

$$C_T = \frac{8}{9} + \left(4Q - \frac{40}{9}\right) a + \left(\frac{50}{9} - 4Q\right) a^2 \tag{3.26}$$

This correction is used when;

$$a > 0.4$$

Differences between the Glauert correction and the Buhl correction, for a state with a tip loss factor of 0.8, are shown in Figure 3.5. As can be seen, there is a gap between the thrust coefficient curve and the Glauert correction, which may cause numerical instabilities in the Blade Element Analysis. In this study, the Buhl correction is used since tip losses are taken into account.

After the induction factors are calculated, sectional force and power values are obtained from;

$$dF = \frac{1}{2}\rho V_1^2 Q\big(4a(1-a)\big)2\pi r dr \quad (3.27)$$

$$dQ = 4aQ(1-a')\rho V_1 \Omega r^3 \pi d\mathrm{r} \quad (3.28)$$

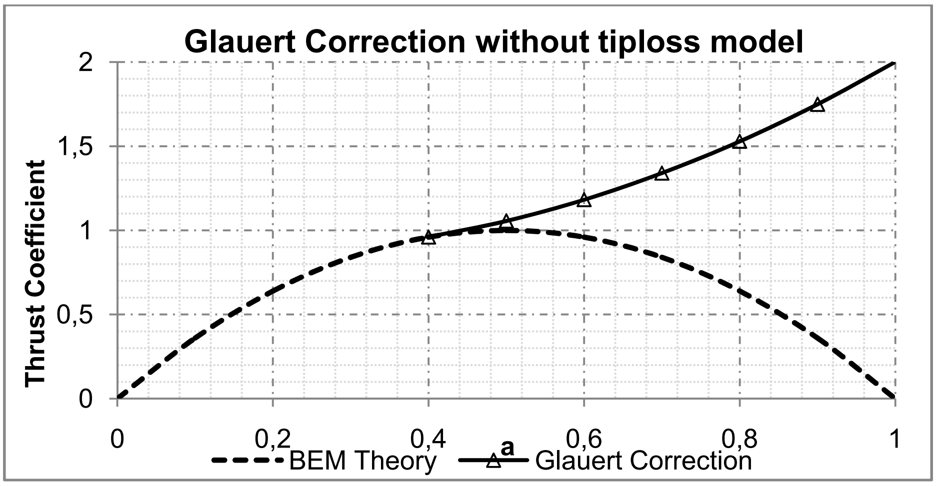

Figure 3.4 Glauert Correction without tip loss model

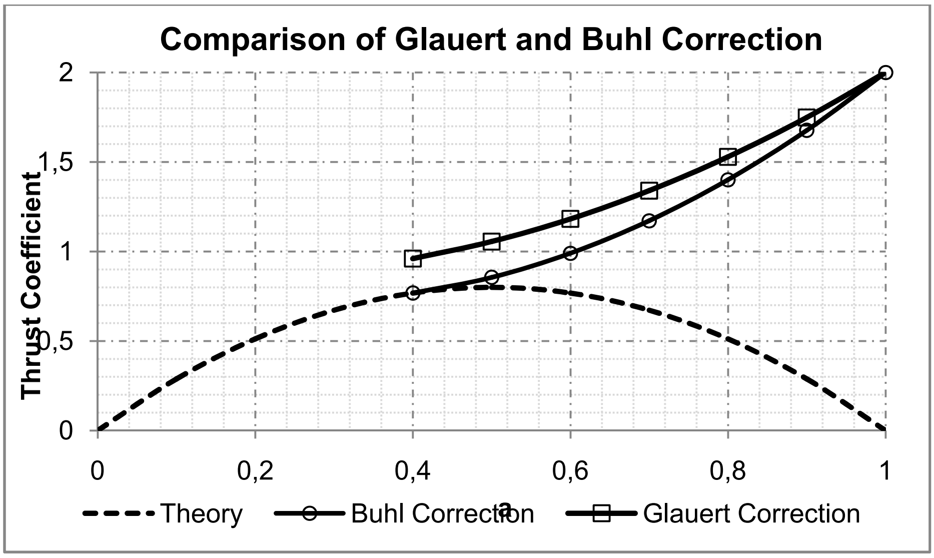

Figure 3.5 Glauert and Buhl corrections compared

3.1.4 The BEM Analysis Tool

As a subroutine of the WindCOE code, the BEM code calculates the power of the wind turbine for a given wind speed. The BEM code uses the Blade Element Momentum Theory equations. The flowchart of the BEM code is shown in Figure 3.6.

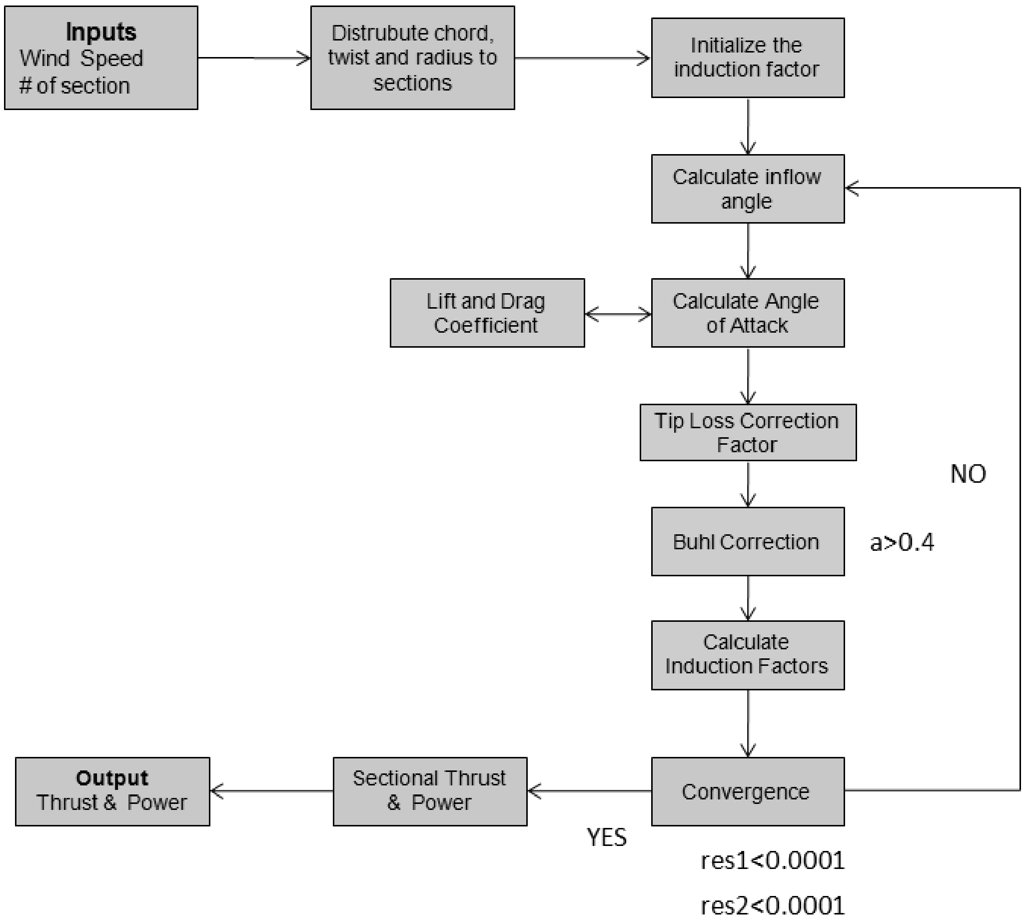

Figure 3.6 BEM Analysis code flowchart

The BEM analysis uses the wind speed and the number of sections as inputs for the analysis. Twist and chord values of each section are calculated by fitting the second order polynomial defined in Chapter 2. The induction factors cannot be calculated directly from equations 3.22 and 3.23, since the inflow angle and aerodynamic coefficients are unknown. Therefore the induction factors are iterated until a convergence is reached. The convergence factor is defined as;

$$res1_i = \left|a_{i,n+1} - a_{i,n}\right| < 10^{-4} \tag{3.29}$$

$$res2_i = \left|a'_{i,n+1} - a'_{i,n}\right| < 10^{-4} \tag{3.30}$$

where i is the section number and n is the iteration number. For the first step, the induction factors are given an initial value of zero. Using these induction factors, the inflow angle is calculated.. The angle of attack is calculated to obtain the lift and drag coefficients corresponding to that state. After Tip Loss Correction factor is calculated according to the axial induction factor, the thrust coefficient is recalculated using Buhl Correction. Induction factors are recalculated using equations 3.22 and 3.23 again. $res1$ and $res2$ are checked for convergence. If residuals are converged, sectional thrust and power are calculated through equations 3.27 and 3.28. Otherwise they are recalculated. Finally, sectional thrust and power values are integrated through the blade span, and the total thrust and power levels are obtained.

3.1.5 Airfoil Profiles

Although airfoil is not used as an optimization parameter in WindCOE, different types of airfoils are evaluated. The airfoil profile distribution along the blade span is selected as an input from one of the two options: either a constant profile distribution or a pre-determined variable profile distribution that is readily available in open literature. In this study we use S809 airfoil for the constant profile option. For the pre-determined variable profiles, two sets of airfoil families are considered depending on the blade length. For rotors with radius smaller than 15m the NREL airfoil family consisting of S814, S815, S825 and S826 is used (Figure 5.3). For rotors with radius larger than 15m the airfoil family consisting of S818, S816 and S817 airfoils is used as recommended in [12]. Since aerodynamic coefficients of selected airfoil profiles are not given in literature, numerical analyses were conducted to obtain them. Details of airfoil profiles and database generation are presented in Chapter 5.

3.1.6 Validation of the BEM Tool

The BEM code is validated against NREL Phase II untwisted, untapered experimental wind turbine [20], in order to prove its accuracy in calculating the power output. Characteristics of the NREL Phase II wind turbine are given in Table 3.1

.

Table 3. 1 NREL Phase II Wind Turbine Specifications

n	3
ω (rpm)	72
r_{tip}(m)	5.03
r_{hub} (m)	0.723
∅ (deg.)	12 (constant)
c_{root} (m)	0.4572
c_{tip} (m)	0.4572
C_l, C_d	S809 airfoil (all sections)

Lift and drag coefficients of the S809 airfoil has been shown in Chapter 5.

Power curve comparison between the results of the BEM code and the experimental data for NREL Phase II Wind Turbine is given in Figure 3.7. As can be seen, the BEM code is agreeing well with the experimental data. Observed differences are mainly because of the three dimensional effects, that are not fully modeled in the BEM code.

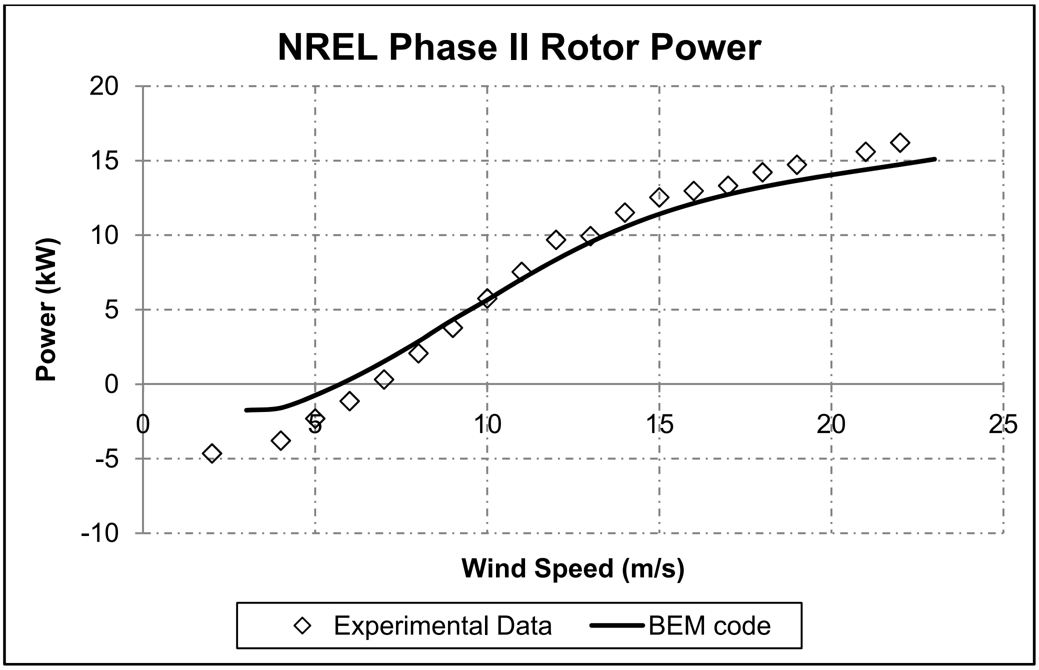

Figure 3.7 Comparison of experimental and BEM code power output

3.2 Weibull Analysis

The mean wind speed information of a wind site is generally not sufficient by itself to estimate the AEP. Instead, the wind speed variation is usually defined by a special probability density function, known as, the Weibull distribution. Weibull distribution of a specific wind site is characterized by a shape parameter *k*, a scale parameter *c*, and the wind speed *U*. The probability density function is defined as,

$$w(U) = \left(\frac{k}{c}\right)\left(\frac{U}{c}\right)^{k-1} exp\left[-\left(\frac{U}{c}\right)^{k}\right] \quad \left(\frac{1}{m/s}\right) \tag{3.31}$$

Weibull probability has to be calculated in a wind speed interval while calculating the AEP. As shown in Figure 3.8, the wind frequency is obtained by computing the area under the Weibull distribution within a predefined wind speed interval.

Although the unit of the Weibull function is — , when it is multiplied with the wind speed (i.e. integrated), it becomes non-dimensional.

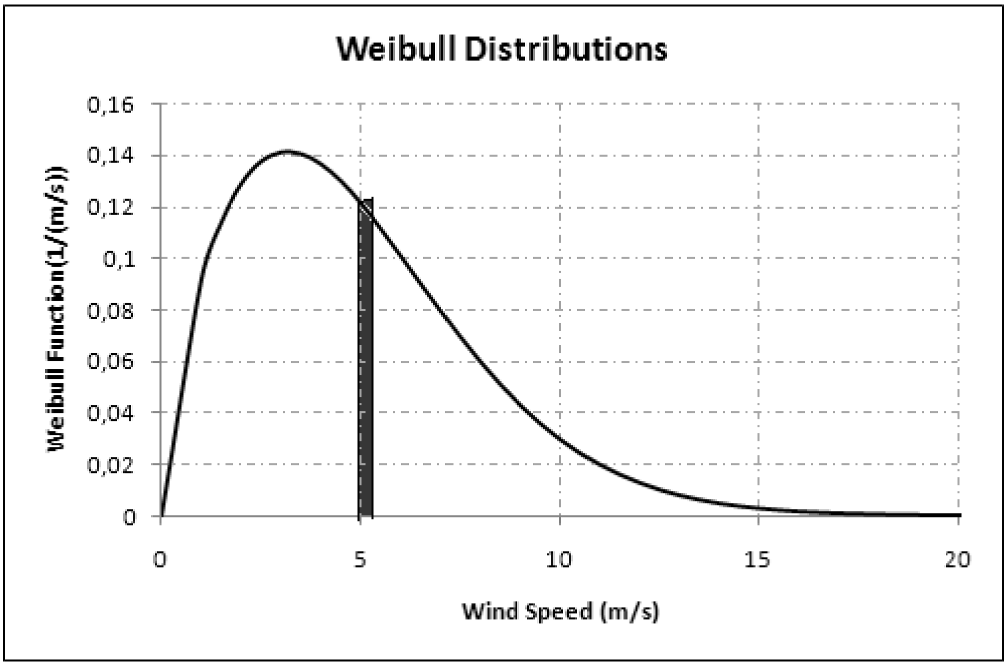

Figure 3.8 Integration of the Weibull function

CHAPTER 4

THE LIFE CYCLE COST MODEL

The Life Cycle Cost (LCC) is the total cost of a wind turbine that covers many items such as the manufacturing costs, material expenses, operation and maintenance costs, annual rent of the wind site, renewal of the wind turbine parts, engineering expenses etc. In this study we use the LCC model developed by NREL [6].

Since the model is constructed partly by using existing commercial wind turbine data, it has some limitations on the application, such as the cost output is in 2002 dollars and it is applicable only for three-bladed, variable speed, upwind wind turbine configurations. Since large scale wind turbine data are used in developing the NREL model, diameters larger than 40m are preferred in the design optimization. Moreover, costs are based on production of 50MW wind farm [6].

The LCC model is comprised of many algebraic equations that are functions of the rotor diameter, the hub height, the rated power and the Annual Energy Production (AEP). A component breakdown of these equations is shown in Figure 4.1. LCC consists of mainly two parts: Initial Capital Cost (ICC) and Annual Operating Expenses (AOE). LCC is calculated as;

$$LCC = FCR * ICC + AOE \quad (\$) \tag{4.1}$$

where FCR is the Fixed Charge Rate, as explained in Chapter 2. ICC is the Initial Capital Cost in dollars and AOE is the Annual Operating Expenses in dollars.

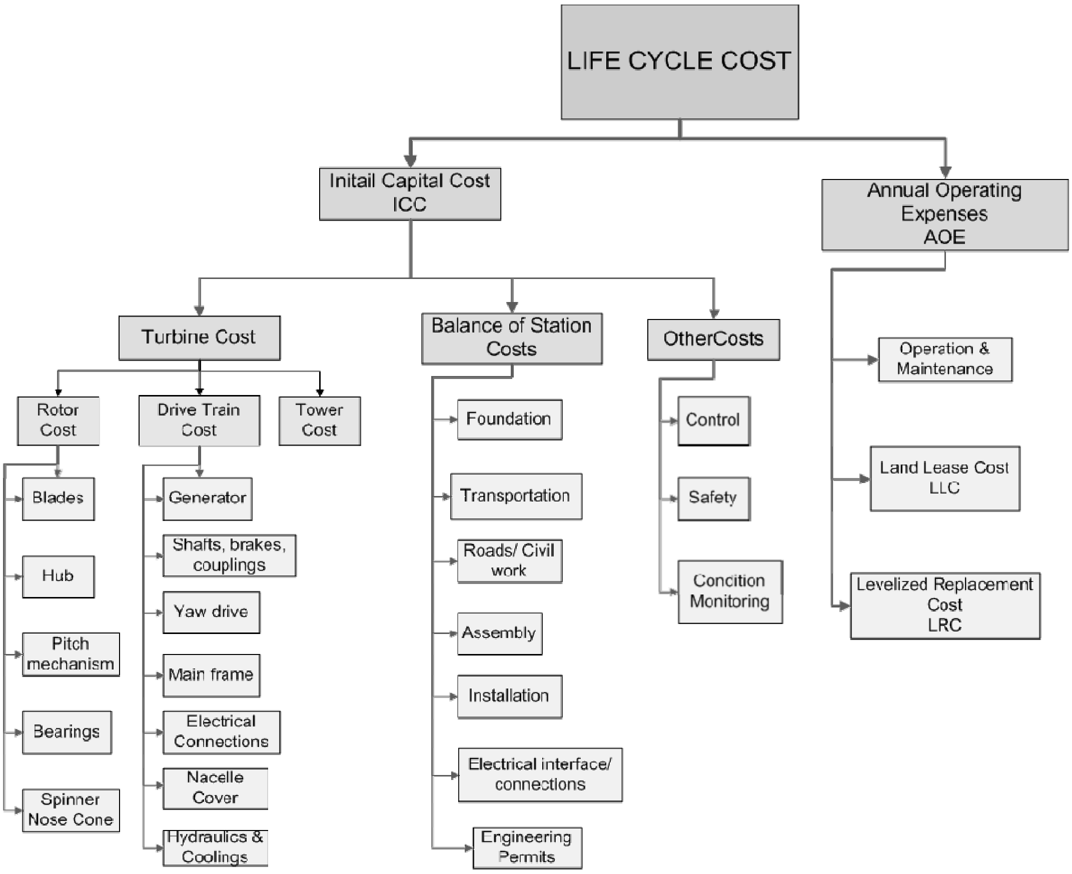

Figure 4.1 Life Cycle Cost model component breakdown

4.1 Initial Capital Cost

The Initial Capital Cost (ICC), one of the main components of LCC, is mainly made up of material, manufacturing, system, and engineering costs. Service costs and financing fees are not included since these are included in the Fixed Charge Rate (FCR). Annual Operating Expenses include costs that are paid every year regularly for operation and maintenance, land rent and replacement of the turbine parts.

4.1.1 Turbine Costs

Turbine costs mainly consist of rotor component costs, drive train costs and tower costs. Algebraic equations for these components are given below.

Blades:

Cost of total three blades, as a function of rotor diameter, is calculated as follows;

$$C_{blade} = 3 * [(0.4019R^3 - 955.24) + 2.7445 * R^{2.5025}]/(1 - 0.28) \quad (4.1.1)$$

Hub:

The cost the hub is calculated as a function of mass. The mass of hub as a function of the mass of the blade is given as;

$$M_{hub} = 0.954 * M_{blade} + 5680.3 \quad (4.1.2.a)$$

Cost of the hub is calculated as follows;

$$C_{hub} = M_{hub} * 4.25 \quad (4.1.2.b)$$

Nose Cone:

Nose cone cost is calculated as a function of the nose cone mass. The mass and the cost of the nose cone are given in the following equations as ;

$$M_{nose} = 18.5 * D - 520.5 \quad (4.1.3.a)$$

$$C_{nose} = M_{nose} * 5.57 \quad (4.1.3.b)$$

Main Bearings:

Cost of the main bearing is calculated as a function of its mass. The mass and the cost of the main bearing are given as;

$$M_{bearing} = \left(D - \frac{8}{600} - 0.033\right) * 0.0092 * D^{2.5} \quad (4.1.4.a)$$

$$C_{bearing} = 2 * M_{bearing} * 17.6 \quad (4.1.4.b)$$

Gearbox:

Cost of the Multi-Path Drive gearbox as a function of rated power is given as;

$$C_{gearbox} = 15.26 * P_{rated}^{1.249} \qquad (4.1.5)$$

Rated power has the unit of kW.

Low speed shaft:

Cost of the low speed shaft as a function of diameter is given as follows;

$$C_{shaft} = 0.01 * D^{2.887} \qquad (4.1.6)$$

Brake, Coupling and associated components:

Cost of the brake associated components like mechanical brake, high-speed coupling etc. are calculated as a function of the rated power as follows;

$$C_{brake} = 1.9894 * P_{rated} - 0.1141 \qquad (4.1.8)$$

Generator:

Cost of the Multi-path Drive with Permanent Magnet Generator is calculated as a function of the rated power as,

$$C_{gen} = P_{rated}*48.03 \qquad (4.1.9)$$

Variable Speed Electronics;

Cost of the variable speed electronics components as a function of the rated power is given as;

$$C_{v\_speed} = P_{rated}*79 \qquad (4.1.10)$$

Yaw Drive System:

Cost of the yaw drive system is given as a function of the rotor diameter as;

$$C_{yaw} = 2 * (0.0339 * D^{2.964}) \qquad (4.1.11)$$

Mainframe:

Cost of the mainframe of the Multi-path Drive with Permanent Magnet Generator is calculated as a function of the rotor diameter as;

$$C_{mf} = 17.92 * D^{1.672} \tag{4.1.12}$$

Electrical Connections:

Cost of electrical connections, which includes switchgear and tower wiring, are calculated as a function of the rated power as;

$$C_{elect} = 40 * P_{rated} \tag{4.1.13}$$

Hydraulics and Cooling System:

Cost of the hydraulics and cooling system is calculated as a function of the rated power as;

$$C_{hyd} = 12 * P_{rated} \tag{4.1.14}$$

Nacelle Cover:

Cost of the nacelle cover is calculated as a function of the rated power as;

$$C_{elect} = 11.537 * P_{rated} + 3849.7 \tag{4.1.15}$$

Tower:

Cost of the tower structure is given as a function its mass. Mass of the tower is given as;

$$M_{tower} = 0.3973 * A_{disk} * h - 1414 \tag{4.1.16}$$

h is the hub height and $A_{disk}$is the rotor disk area. Cost of the tower is given as;

$$C_{tower} = 1.5 * M_{tower} \tag{4.1.17}$$

Cost breakdown for the turbine components are shown in Figure 4.2. As can be seen biggest portion of the cost belongs to drive train components.

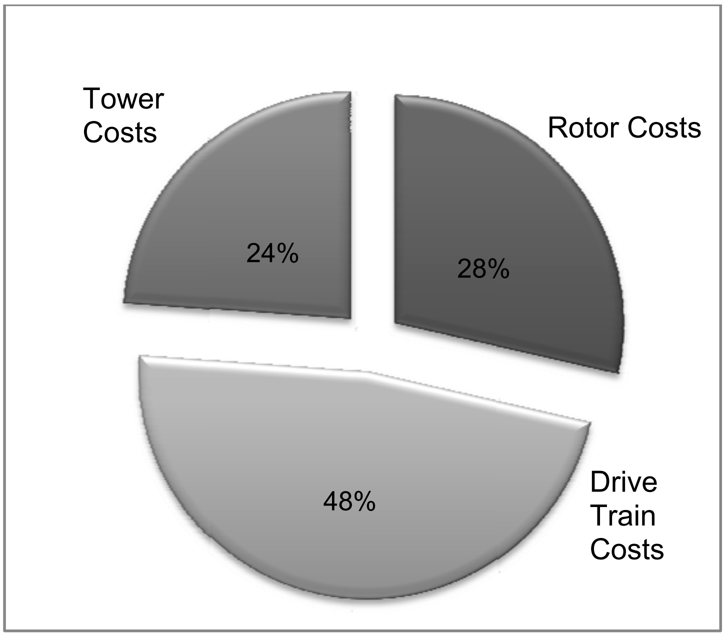

Figure 4.2 Cost breakdown for the wind turbine components

4.1.2 Balance of Station Costs

Balance of Station of costs include the expenses of services from manufacturing to operation of a wind turbine. It includes transportation of wind turbine components, construction of foundation, construction of roads and other civil work for the transportation, assembly and installation of the wind turbine. Algebraic cost equations of balance of station are given below.

Foundation:

Cost of the foundation is given as a function of the disk area and hub height as;

(4.1.18)

Transportation:

Cost of the transportation to carry all structure to wind site area is given as a function of the rated power as;

$$F_{trans} = 1.581E - 05 * P_{rated}^2 - 0.0375 * P_{rated} + 54.7 \quad (4.1.19.a)$$

$$C_{trans} = 40 * F_{trans} \quad (4.1.19.b)$$

Roads, Civil Work:

Roads and civil work include the costs for construction of roads and other civil work to transport the wind turbine structure to wind site. Costs of the roads and civil work are given as a function of the rated power as;

$$F_{civil} = 40 * P_{rated}^2 - 0.0145 * P_{rated} + 69.54 \quad (4.1.20.a)$$

$$C_{civil} = P_{rated} * F_{civil} \quad (4.1.20.b)$$

Assembly and Installation:

Cost of the assembly and installation of the wind turbine is given as a function of the hub height and the rotor diameter as;

$$C_{assem} = 1.965 * (h * D)^{1.1736} \quad (4.1.21)$$

Electrical and Interference Connections:

Cost of the electrical interface and connections are calculated as a function of the rated power as;

$$F_{inter} = 3.49E - 06 * P_{rated}^2 - 0.0221 * P_{rated} + 109.7 \quad (4.1.21.a)$$

$$C_{inter} = P_{rated} * F_{inter} \quad (4.1.21.b)$$

Engineering and Permits:

Engineering and permits covers the cost of engineering expenses during design and manufacturing processes, and permissions for designing entire wind facility [6]. Cost of the engineering permits as a function of rated power is given as;

$$F_{eng}=9.94E\text{-}04*P_{rated}+20.31 \quad (4.1.22.a)$$

$$C_{eng}=P_{rated}*F_{eng} \quad (4.1.22.b)$$

4.1.3. Other Costs

Other costs include subsystems needed for safe operation of a wind turbine.

Control, Safety System, Condition Monitoring:

Cost for the control, safety system and condition monitoring are given as a constant amount according to application as;

10000 $ for on-shore application

55000 $ for off-shore application

Cost breakdown for the Initial Capital Cost is given in Figure 4.3.

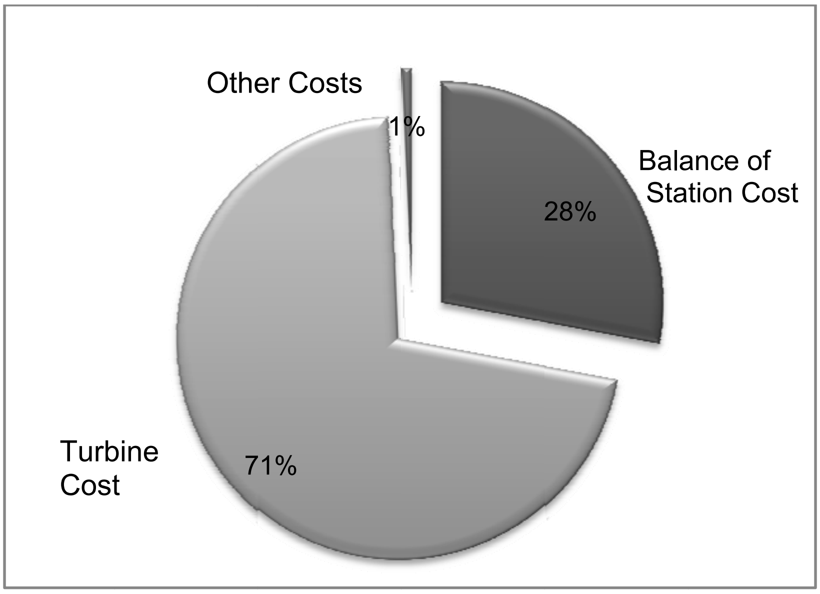

Figure 4.3 Cost breakdown for the Initial Capital Cost

As can be seen from the Figure 4.3 biggest share belongs to turbine costs.

4.2 Annual Operating Expenses

Annual Operating expenses cover the costs for the services that are paid annually. AOE components are Levelized Replacement Costs, Levelized Operation and Levelized Maintenance Costs and Land Lease Costs. Algebraic equations for these components are given below. Levelized value defines total cost over power system's economic life, converted to equal annual payments.

Levelized Replacement Cost:

Levelized Replacement Cost covers the annual expenses of the long-term replacement and overhaul of major wind turbine parts [6]. LRC is constructed as a constant per generated kW as;

$$F_{LRC} = \$10.7/kW \tag{4.2.1.a}$$

$$C_{LRC} = P_{rated} * F_{LRC} \tag{4.2.1.b}$$

Levelized Operation and Maintenance Cost:

Operation and maintenance costs are the annual expenses for scheduled and unscheduled maintenance and operation of a wind turbine. O&M Cost is a function of AEP and calculated as;

$$C_{O\&M} = 0.007/kWh * AEP \tag{4.2.2}$$

Levelized Land Lease Cost:

Land Lease Cost (LLC) is the annual rent paid for a unit turbine. LLC is calculated as a function AEP as;

$$C_{LLC} = 0.00108\ /kWh * AEP \tag{4.2.3}$$

Cost breakdown for Annual Operating Expenses is shown in Figure 4.4. As can be seen, biggest share belongs to the Operational and Maintenance costs.

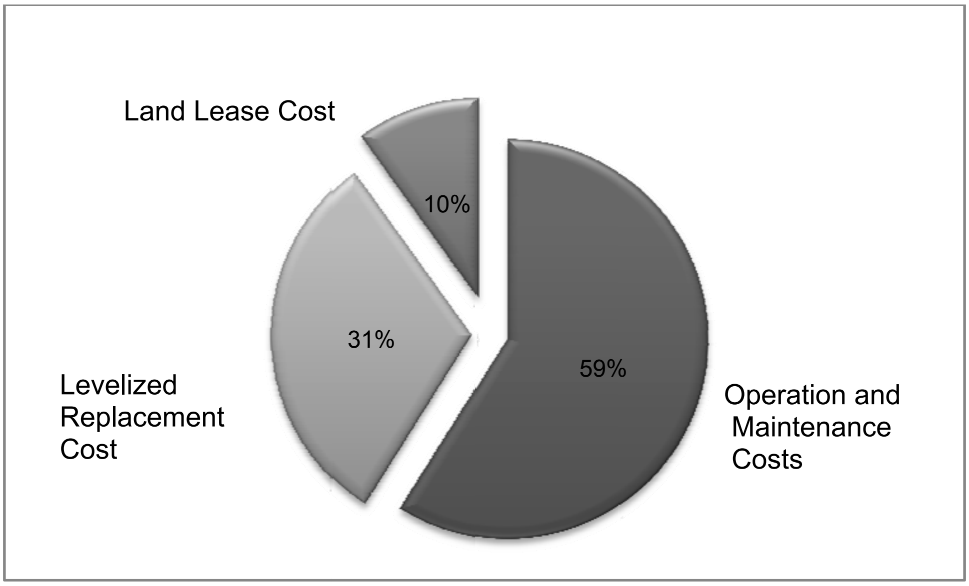

Figure 4.4 Cost breakdown for the Annual Operating Expenses

4.3 Additional Cost Elements for Offshore Applications

Off-shore application of wind turbines bring-in additional cost components.

Marinization:

Marinization includes costs related to extra protection that is necessary for offshore ocean environment like special paintings and coverings, extra sealing for electronic parts etc. Cost of marinization is calculated as a function of total turbine and tower costs as;

$$C_{marin} = 13.5 \text{ of Turbine and tower costs} \qquad (4.3.1)$$

Offshore Transportation:

Offshore transportation means transportation of wind turbine components from shore to sea bed where turbine will be installed. Cost of offshore transportation is calculated as a function of the rated power as;

$$F_{offtrans} = 1.581E - 06 * P_{rated}^2 - 0.0375 * P_{rated} + 54.7 \quad (4.3.2.a)$$

$$C_{offtrans} = P_{rated} * F_{offtrans} \quad (4.3.2.b)$$

<u>Offshore Support Structure:</u>

Offshore support structures are different than onshore based supports since offshore supports have to extend through the base of the ocean. Cost of an offshore support structure can be calculated as a function of the rated power as;

$$C_{support} = 300 * P_{rated} \quad (4.3.3)$$

<u>Port and Staging Equipment:</u>

Special port and staging equipments are needed to service the offshore installation and maintain [6]. Cost of the port and staging equipment, is given as a function the rated power as;

$$C_{stage} = 20 * P_{rated} \quad (4.3.4)$$

<u>Offshore Installation:</u>

Cost of the offshore wind turbine installation is given as a function of the rated power as;

$$C_{offins} = 100 * P_{rated} \quad (4.3.5)$$

<u>Offshore Electrical Interface and Connection:</u>

Cost of the offshore electrical interface and connection is given as a function of the rated power as;

$$C_{offelec} = 260 * P_{rated} \quad (4.3.6)$$

<u>Offshore Engineering Permits and Site Assessment:</u>

Cost of the offshore engineering permits and site assessment is given as a function of the rated power as;

$$C_{offeng} = 37 * P_{rated} \quad (4.3.7)$$

Personnel Access Equipment:

Personal access equipments are vehicles to access offshore site area for servicing like small boats, helicopters, marine vessels. Cost of the personal access equipment is a constant as;

$$C_{offaccess} = \$60000/\ turbine \quad (4.3.8)$$

Scour Protection:

Scour protection is a mechanism that prevents the base of the structure from failure caused by scour. Cost of the scour protection is calculated as a function of the rated power as;

$$C_{scour} = 55 * P_{rated} \quad (4.3.9)$$

Surety Bond:

Surety bond is a type of funding that guarantees removal of unused old or damaged structures. Surety bond is calculated as;

$$C_{surety} = 3\ \%\ (ICC_{offshore} - offshore\ warranty) \quad (4.3.10)$$

Offshore Warranty

Since offshore wind turbines are operated in an extreme environment, extra warranty is needed compared to onshore applications. Cost of the offshore warranty is calculated as;

$$C_{support} = 15\ \%\ (Cost\ of\ turbine\ and\ tower) \quad (4.3.11)$$

Offshore Levelized Replacement Cost:

Offshore LRC is calculated as a function of the rated power as;

$$C_{offLRC} = 17/kW * P_{rated} \quad (4.3.12)$$

Offshore Levelized Bottom Lease Cost:

Offshore Bottom Lease Cost (BLC) is calculated as a function of AEP as;

$$C_{BLC} = 0.00108/kWh * AEP \quad (4.3.13)$$

Offshore Levelized Operating and Maintenance:

Offshore O&M costs are calculated as;

$$C_{O\&M} = 0.02/kWh * AEP \quad (4.3.14)$$

CHAPTER 5

GENERATION OF THE AIRFOIL AERODYNAMIC DATA

In BEM Theory, the sectional forces have to be calculated through lift and drag coefficients, which are characteristics of an airfoil profile. Airfoil is the two dimensional geometry of the blade sections that is able to generate aerodynamic forces. Geometrical parameters that define airfoil characteristics are shown in Figure 5.1

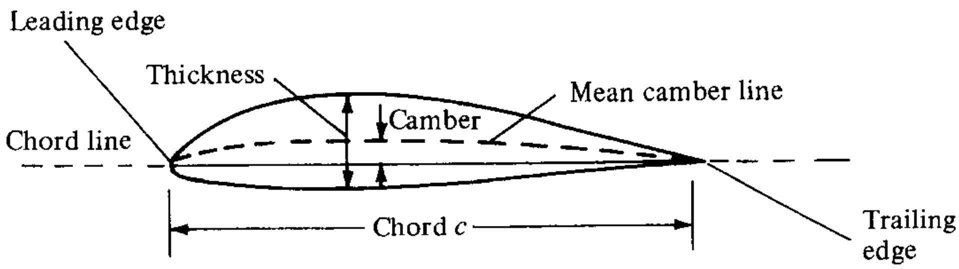

Figure 5.1 Airfoil nomenclature [21]

The lift and drag are components of the force perpendicular and parallel to flow direction, respectively. Forces and moments per unit span are calculated as shown below;

$$L' = \frac{1}{2} C_l \rho U^2 c \tag{5.1.a}$$

$$D' = \frac{1}{2} C_d \rho U^2 c \tag{5.1.b}$$

$$M' = \frac{1}{2} C_m \rho U^2 c r \tag{5.1.c}$$

Lift, drag and moment coefficient characteristics of an airfoil are determined by its shape as defined in Figure 5.1, length and flow characteristics such as velocity, temperature, viscosity and density. Reynolds number is the non-dimensional representation that defines force and moment characteristics. Reynolds number is defined as;

$$Re = \frac{\rho U c}{\mu} \tag{5.2}$$

ρ is the density, U is the flow velocity, c is chord of the airfoil and μ is the kinematic viscosity of the fluid. Reynolds number is the key parameter in choosing an airfoil for a specific application.

In order to have good lift and drag characteristics on a rotor blade, which will in turn generate good power output, airfoils should be chosen according to application characteristics. Before wind turbine specific airfoils were designed, airfoils that are used in helicopters and aircraft were utilized also in wind turbines, which naturally resulted in poor power performance. In wind turbine applications parameters that should be considered when choosing an appropriate airfoil are the Reynolds number and roughness sensitivity. Since, especially large wind turbines experience varying flow conditions from root to tip of the rotor, different airfoils might be chosen according to the spanwise location.

5.1 Airfoil Database

NREL has developed an airfoil series [12], which are specifically designed for wind turbine applications considering the problems that reduce power. Since, soiling effects decrease the maximum lift coefficient on a blade, the total amount of energy produced also decreases. By designing airfoils that are insensitive to roughness, NREL was able to increase total energy produced up about 15%. Moreover by designing airfoils specific to a spanwise location on the blade, NREL has obtained optimized airfoils with respect to Reynolds number. This optimization has resulted in an increase in performance about 3 to 5 %.

Performance improvement of NREL Airfoil series compared to previously used airfoil families is shown in Table 5.2.

Table 5.1 Estimated annual energy improvements from NREL airfoils [12]

Turbine Type	Roughness Insensitive $c_{l,max}$	Correct Reynolds Number	Low Tip $c_{l,max}$	Total Improvement
Stall-Regulated	10% to 15%	3% to 5%	10% to 15%	23% to 35%
Variable-Pitch	5% to 15%	3% to 5%	---	8% to 20%
Variable-RPM	5%	3% to 5%	---	8% to 10%

Designed airfoils are for an application range from 15m to larger in radius. For blades with length 10m to 15 meters, NREL S-Series airfoil family consisting of S814, S815, S825 and S826 is used as shown in Figure 5.2. For blades larger than 15 meters NREL S-series airfoil family consisting of S818, S816 and S817 airfoils is used as shown in Figure 5.3.

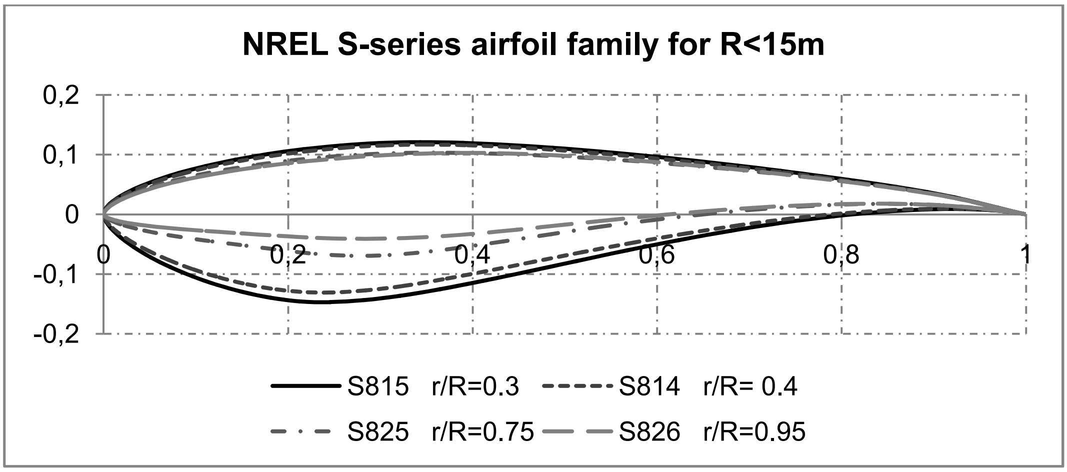

Figure 5.2 Geomety of the S815, S814, S825 and S826 airfoils

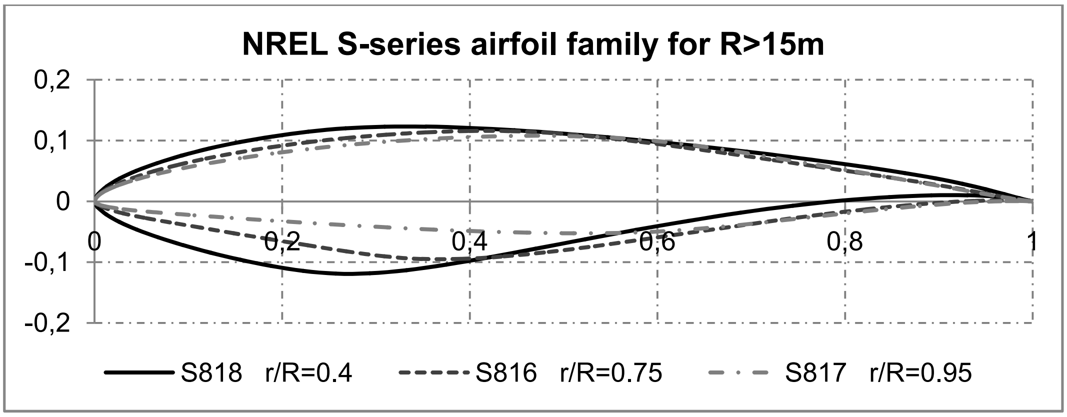

Figure 5.3 Geometry of the S818, S816 and S817 airfoils

5.2 Numerical Analysis of the Airfoils

Aerodynamic characteristics of the NREL S-series airfoil families are not available in open literature. Therefore, numerical analyses of the airfoils were conducted to obtain lift and coefficients. Two-dimensional Navier-Stokes equations are solved using FLUENT commercial solver. The mesh was created as a C-type grid, and was created using commercial mesh generator GAMBIT.

5.2.1 Validation Case for Numerical Analysis

As a validation case, the S809 airfoil profile whose aerodynamic characteristics are well-known through various wind tunnel tests was analyzed. After the validation of the S809 airfoil, other airfoils are analyzed similarly in terms of mesh and solver characteristics. Sectional geometry of the S809 airfoil is shown in Figure 5.4.

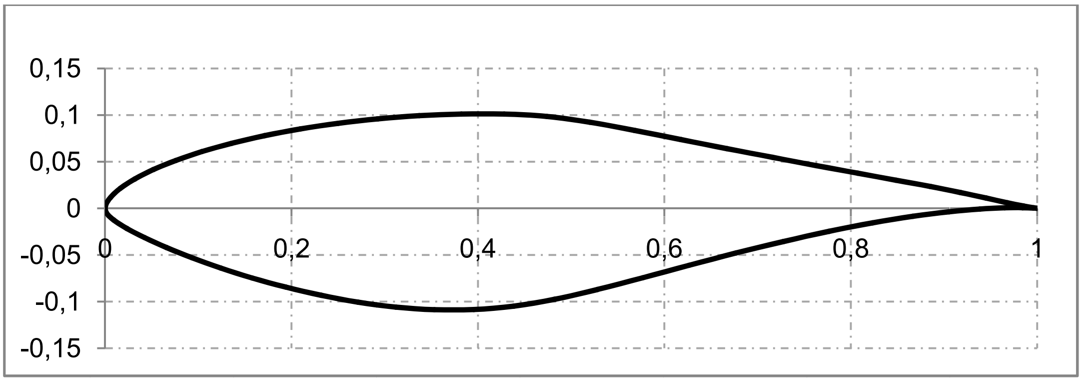

Figure 5.4 S809 airfoil geometry

A C-type structured mesh is created using the commercial mesh generator GAMBIT consisting of 12000 elements in total are generated. The first grid point is 10^{-6} m away from the surface. This was small enough to be able to resolve the viscous sub-layer (y^+=1).The computational mesh used for S809 airfoil simulations is shown in Figure 5.5.

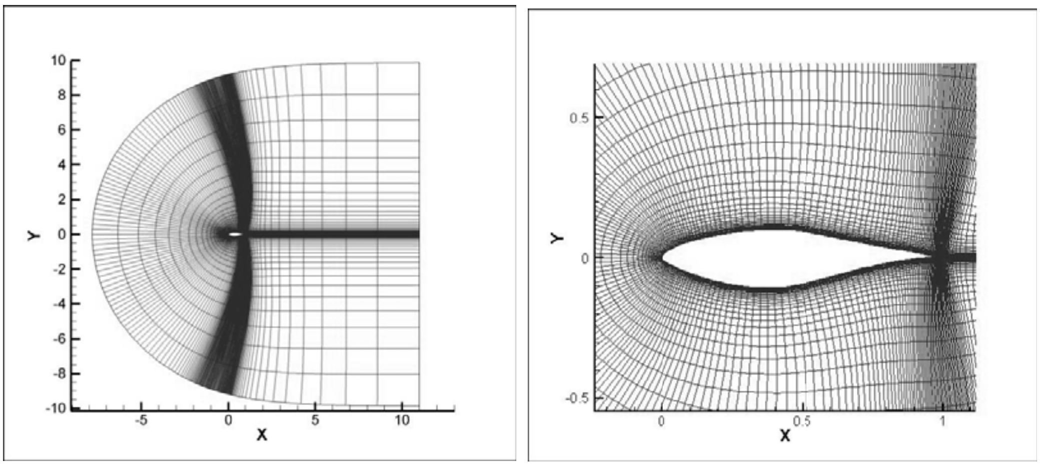

Figure 5.5 2-D structured C-type computational S809 airfoil

For the validation test case, the solutions are obtained at Reynolds number of 1 million. Density based solver is used as FLUENT solver settings. As a turbulence model Spalart- Allmaras is selected.

Results are compared against the wind tunnel measurements performed at the from Ohio State University (OSU) [20] and Delft University of Technology (DUT) [20] as shown in Figure 5.6 (a) and (b).

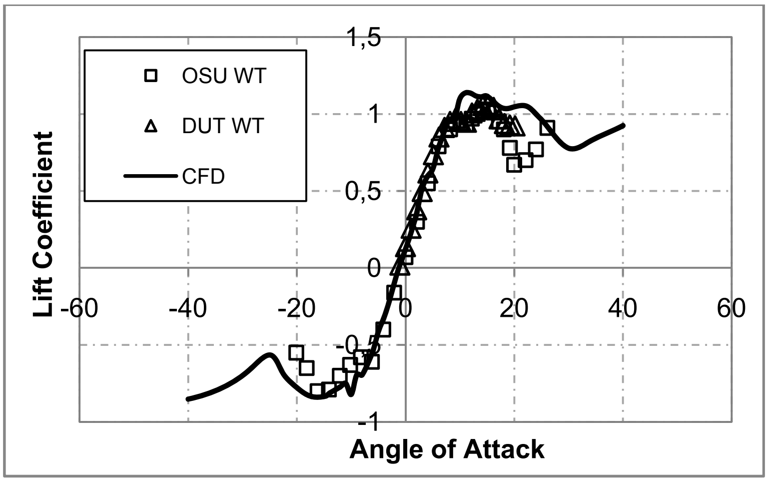

(a)

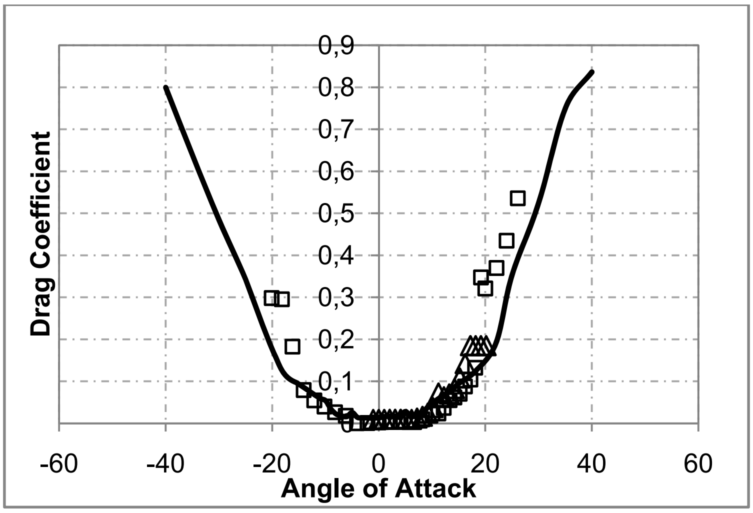

(b)

Figure 5.6 (a) Lift and (b) drag coefficient comparisons of the numerical results with the experimental data

As can be seen from Figure 5.6, both the computed lift and drag coefficients fit the wind tunnel data up to 12 degrees angle of attack. After this angle there is some shift in both coefficients possibly due to the separation which cannot be modeled accurately.

Resultant lift and drag coefficients of NREL S-series airfoils are given in Appendix A.

The lift and drag coefficients for the airfoil sections are obtained in a limited angle of attack range (-40^0 to 40^0) due to convergence related problems in CFD simulations. Since wind turbine blades may operate at extremely high angle of attack values, the aerodynamic coefficients should generally be presented in an angle range of -180^0 to $+180^0$. The C_l and C_d results are extrapolated to the -180^0 to $+180^0$ range using Airfoil_Prep [22], which is an open source code provided by NREL and utilizes the Viterna method. This method is based on calculating post stall characteristics of the airfoil and is able to estimate the aerodynamic coefficients at higher angles. Extrapolated lift and drag coefficients of S809 airfoil are shown in Figure 5.7.

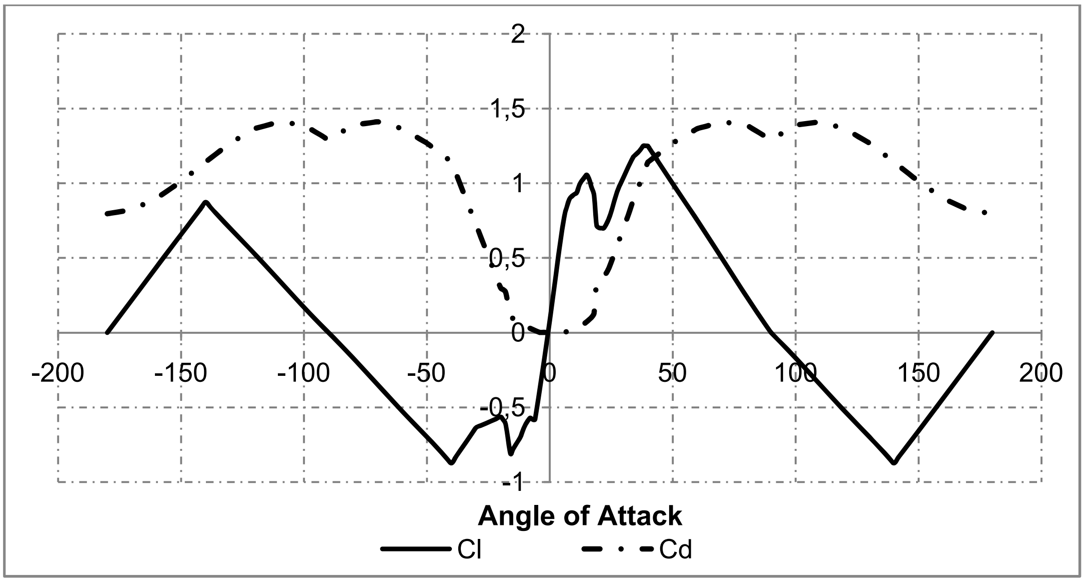

Figure 5.7 Extrapolated aerodynamic data of S809 airfoil

Representation of the Aerodynamic Data using Neural Network

The data for the aerodynamic coefficients that are generated by the computational analysis are implemented to the BEM routine through an Artificial Neural Network.

Neural Networks are rapid data creators based on parallel unit processors. Data is created in two steps. In the first step, which is the training by storing certain input of data, algorithm creates a database. Using that database, algorithm learns characteristics of the variation of the data and creates a list of weighting coefficients for it. In the second step, using these weighting coefficients, the Neural Network can estimate the value of the data for any input given. Neural Network is preferred due to its high accuracy and rapid data processing capability. In this study, multi-layer feed forward type Neural Network is used [23].

The training process is based on two hidden layers. Numbers of neurons used in these layers are: 11 in the first layer and 13 in the second layer. Convergence is reached when the steady state error is less than 10^{-5}. Figure 5.8 shows the original extrapolated C_L-α variation and its Neural-Network representation. As is evident, the representation is quite satisfactory.

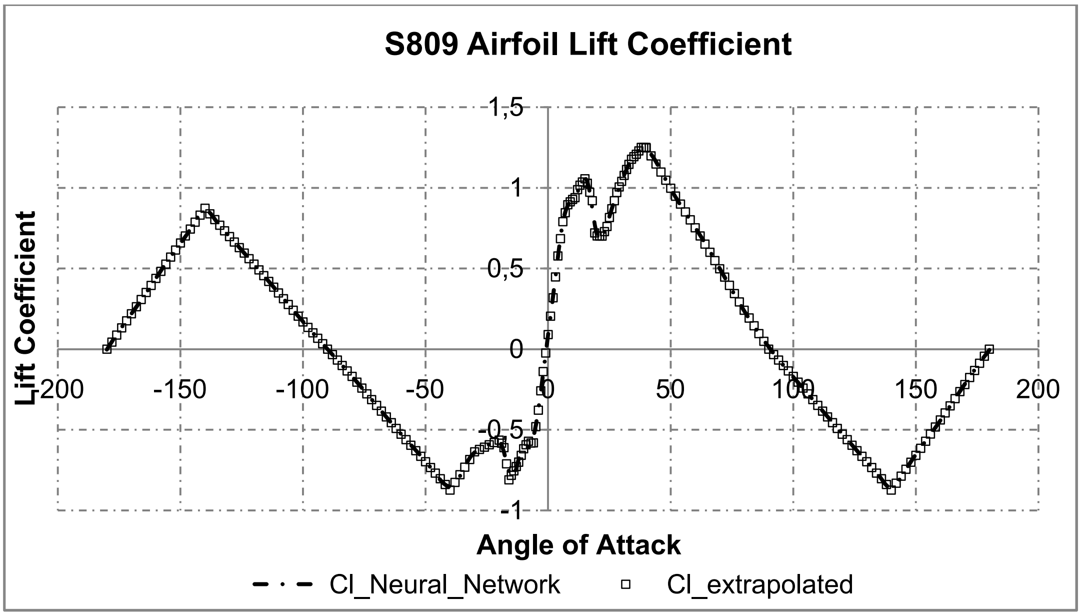

Figure 5.8 Comparison of the extrapolated and the NN representation of the lift coefficient for the S809 airfoil

Numerical analyzes are conducted for all airfoils. Reynolds numbers that analyses are performed are the design Reynolds number of airfoils given in [12]. Except from Reynolds number, all the flow properties are given same with S809 flow characteristics.

CHAPTER 6

RESULTS AND DISCUSSION

In this chapter, initially, selected wind sites on which wind turbines are designed, are presented with their wind speed characteristics. Design optimization studies are performed on baseline designs whose characteristics and performance are given. Three different scenarios are generated to investigate the effect of various airfoil profiles and rated power on each of the selected wind sites. Finally, resultant optimization parameters and performance parameters such as Cost of Energy and Annual Energy Production are presented for each design.

6.1 Selected Wind Sites

Three different wind sites, including onshore sites from various regions of Turkey and offshore from Germany, have been selected to demonstrate the effect of the wind characteristics on Cost of Energy. These are a low wind speed site near İskenderun [24], a high wind speed site in Gökçeada [25] and a offshore site at Germany-North Sea [26]. The offshore site generally has a higher mean wind speed due to less skin friction and less surface roughness. Weibull characteristics and distributions of the selected wind sites are shown in Table 3.2 and Figure 3.9, respectively. Weibull characteristics of sites are taken from literature.

Table 6.1 Weibull Characteristics of selected sites.

	Low Wind Speed Site Iskenderun [24]	High Wind Speed Site Gokceada [25]	Offshore Site Germany-North Sea [26]
k	0.78	1.7	2.26
c* *[1/(m/s)]	4.8	9.86	11.2

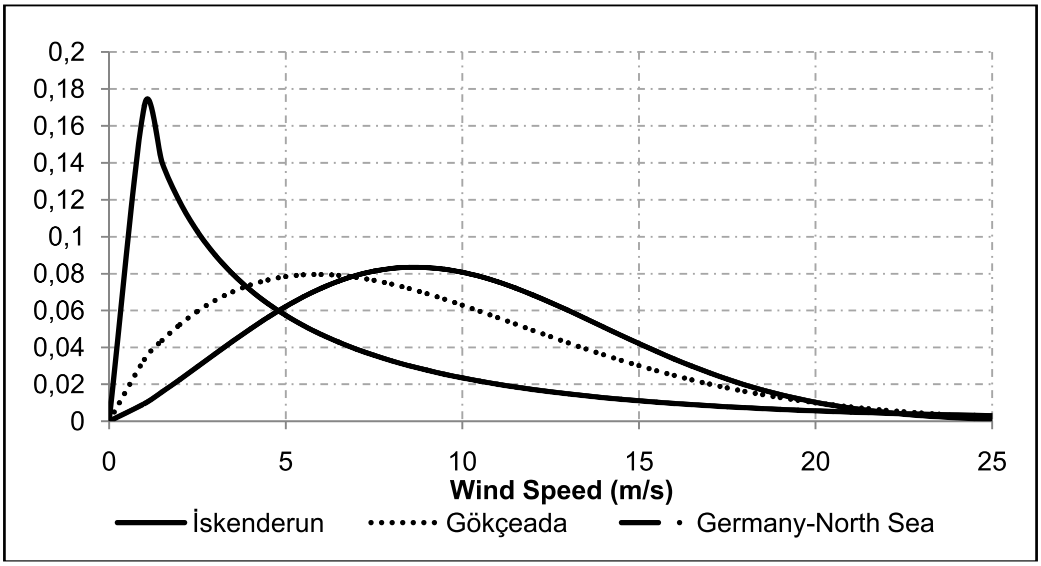

Figure 6.1 Weibull Distributions of selected sites

6.2 Baseline Designs

The design optimization study is performed on a baseline configuration, which is selected as a three-bladed, upwind, fixed-pitch and variable speed HAWT. This is one of the widely used configurations in wind turbine industry [2]. The design of the baseline configuration is achieved using **WindCOE** without performing the optimization process. Selected design parameters for the baseline configuration are tabulated in Table 6.2.

Table 6.2 Baseline Design Characteristics

BASELINE DESIGN	
r_{tip}(m)	40
r_{hub} (m)	2
P_{rated}(MW)	1.7
TSR	7
$\emptyset_{root}$ (deg.)	15
$\emptyset_{mid}$ (deg.)	8
$\emptyset_{tip}$ (deg.)	0
c_{root} (m)	3.0
c_{mid} (m)	2.0
c_{tip} (m)	0.4
C_l, C_d	S809 airfoil (all sections)

The diameter of the baseline design is selected as 80 m, due to the fact that cost model is valid only for rotors that are larger than 40 m. This value is also a typical size in wind turbine market. The rated power of the baseline design is calculated as 1.7MW using Equation 2.4. The Tip Speed Ratio (TSR), which is the ratio between rotational speed of the tip of the blade and the wind velocity, is selected as 7, which is also a typical value for modern wind turbines [2].The chord and twist values are selected according to the same size commercial wind turbines [16] and S809 airfoil profile is used for all sections of the baseline.

The COE and AEP values of the baseline configuration are evaluated for the three selected wind sites, i.e. İskenderun (Low Wind Site), Gökçeada (High Wind

Site) and Germany- North Sea (Offshore Site), for which the Weibull distributions are presented previously in Chapter 3. The results are presented in Table 6.3

Table 6.3 COE and AEP outputs of Baseline Design

	Low Wind Site (İskenderun)	**High Wind Site (Gökçeada)**	**Offshore Site (Germany North Sea)**
AEP (MWh)	2318.3	5356.2	6676.8
COE (cents/kWh)	10.83	5.88	5.14

As seen from Table 6.3, wind turbine designed for the offshore site has the minimum COE, mainly due to the high wind speed profile which results in a higher AEP. Wheras, baseline wind turbine extracts much less energy in the low wind site due to the decreased levels of wind speed and hence results in a higher COE value.

6.3 Design Optimization Scenarios

A series of design optimization runs are performed on the baseline HAWT, to investigate the effects of various parameters on the COE. Three different optimization scenarios are conducted for each and every one of the selected wind sites. The first scenario uses the same airfoil profile (S809) through all sections of the blade and the optimization parameters are selected as the chord and twist distribution that are represented by the root, mid and tip values on the blade as explained in Chapter 3. The second scenario performs a similar design optimization; however, NREL S-series airfoil family is used on the rotor blade. For the third scenario, the rated power is also used as an optimization parameter in addition to the chord and twist distributions. NREL S-series airfoil family is also used for the third optimization scenario. A summary of the design optimization scenarios applied for of the selected wind sites are tabulated in Table 6.4.

Constraints for the optimization parameters are determined according to the baseline design parameters as shown in Table 6.5.

Table 6.4 Design Optimization Scenarios for the low, high and offshore wind sites. Each scenario is studied for each and every one of the selected wind sites.

SCENARIO 1 (S1)		SCENARIO 2 (S2)		SCENARIO 3 (S3)	
Optimization Parameters	**Airfoil Profile**	**Optimization Parameters**	**Airfoil Profile**	**Optimization Parameters**	**Airfoil Profile**
Chord Twist	S809	Chord Twist	S816 S817 S818	Chord Twist Rated Power	S816 S817 S818

Table 6.5 Optimization parameter limits

	θ_{root} (deg.)	θ_{mid} (deg.)	θ_{tip} (deg.)	c_{root} (m)	c_{mid} (m)	c_{tip} (m)	P_{rated} (MW)
Lower Limit	0	-10	-20	2.4	1.6	0.32	1.5
Upper Limit	40	30	20	3.6	2.4	0.48	1.9

Chord and rated power limits are selected as $\pm 20\ \%$ and $\pm 10\ \%$ of the baseline design values, respectively. Since the twist value does not affect the structural weight and loads as much as chord, its limits are selected as maximum and minimum twist values of any size wind turbine that commercially exists. Chord limits are shown in Figure 6.2. Additionally, blade area is also limited to 72m^2 based on similar size commercial wind turbine. [16]

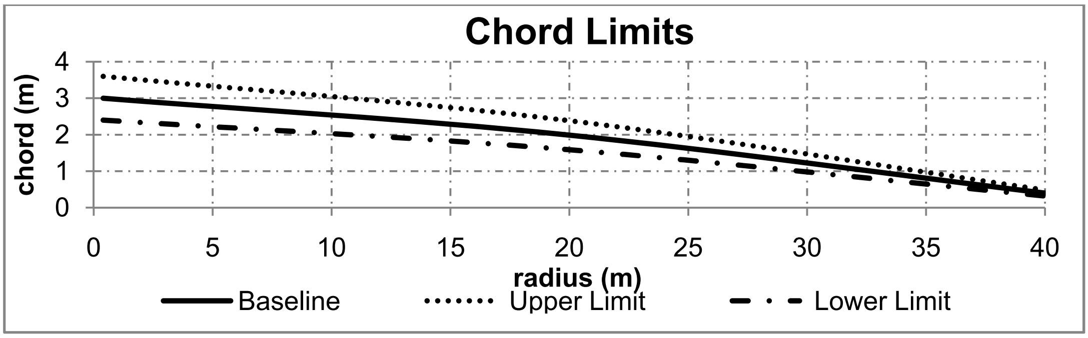

Figure 6.2 Upper and lower optimization limits for the blade chord

6.4 Optimization Results

6.3.1 Results of the Design Optimization Scenarios

Scenario 1

S1 tries to find optimum chord and twist at root, mid and tip of the blade based on baseline design. The S809 airfoil is used at all blade sections. Resultant optimization and performance parameters are shown in Table 6.6 and Table 6.7, respectively.

Table 6.6 Resultant Optimization Parameters for S1

	θ_{root} (deg.)	θ_{mid} (deg.)	θ_{tip} (deg.)	c_{root}(m)	c_{mid}(m)	c_{tip}(m)
Low Wind Site	20.55	6.5	2.2	3.22	2.4	0.48
High Wind Site	25.6	6.9	1.4	3.35	2.4	0.48
Offshore Site	25.9	7.0	0.8	3.12	2.4	0.48

Although tip and mid chord values reach the maximum of their limits, root chord does not. This is due to blade area constraint. Since less lift is obtained from root of the blade, which is because of low sectional rotational speed the code limits the root chord instead of tip section.

Table 6.7 Design Optimization Results for S1

	AEP (MWh)	COE (cents/kWh)	LCC/LCC_{BL}	AEP/AEP_{BL}	COE/COE_{BL}
Low Wind Site	2577.3	9.96	1.022	1.111	0.91938
High Wind Site	6130.4	5.41	1.053	1.145	0.91969
Offshore Site	7746.5	4.72	1.065	1.160	0.91820

As can be seen from the Table 6.7, low wind site has the maximum COE and the offshore site has the minimum COE. Conversely, AEP is the minimum for the low wind site and the maximum for the offshore wind site. These results are expected since potential of generating energy is higher for offshore site due to high wind speed characteristics.

Comparison with baseline configuration is represented by LCC/LCC_{BL}, AEP/AEP_{BL} and COE/COE_{BL}. LCC/LCC_{BL} rates show that LCC is higher compared to baseline configuration, since LCC is a function of AEP and AEP is improved compared to baseline configuration for all wind sites. Moreover, AEP/AEP_{BL} and COE/COE_{BL} results indicate that AEP is increased and COE is decreased compared to the baseline configuration for all wind sites, which means an improvement in objective function, COE, is achieved.

Twist and chord distributions for Scenario1 are also shown in Figure 6.3.a and 6.3.b, respectively.

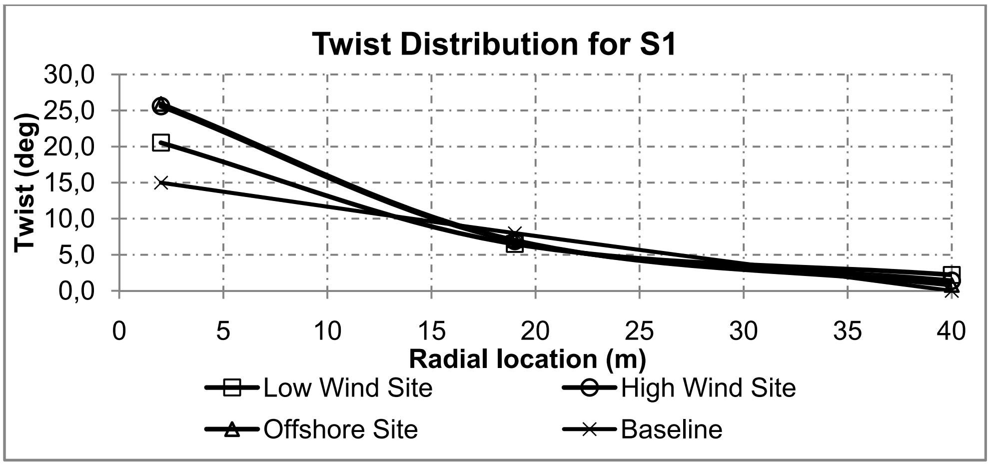

(a)

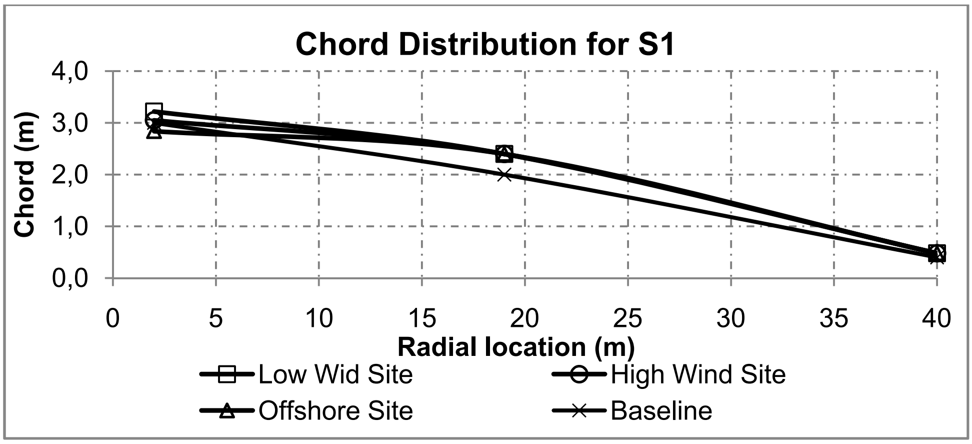

(b)

Figure 6.3 Resultant (a) Twist and (b) Chord distribution for S1

Scenario 2

S2 is similar to S1 except that the airfoil profiles are the NREL S-series airfoil family. Resultant optimization parameters and performance parameters for the S2 are shown in Table 6.8 and Table 6.9, respectively.

Table 6.8 Resultant Optimization Parameters for S2

	θ_{root} (deg.)	θ_{mid} (deg.)	θ_{tip} (deg.)	c_{root} (m)	c_{mid} (m)	c_{tip} (m)
Low Wind Site	27.7	5.1	0.2	3.05	2.4	0.48
High Wind Site	27.7	5.8	-0.9	3.01	2.4	0.48
Offshore Site	29.4	6.1	0.3	2.82	2.4	0.48

Table 6.9 Design Optimization Results for S2

	AEP (MWh)	COE (cents/kWh)	LCC/LCC_{BL}	AEP/AEP_{BL}	COE/COE_{BL}
Low Wind Site	2710.2	9.57	1.033	1.169	0.8839
High Wind Site	6307.7	5.32	1.064	1.177	0.9039
Offshore Site	7884.2	4.67	1.074	1.181	0.9093

Trends of the optimization parameters are similar to S1. Chord values at mid and tip regions converge to the upper limit, whereas the root chord is restrained by the blade area constraint.

AEP and COE parameters are improved from low wind site to offshore site as seen from Table 6.9. Similar to S1 results, LCC and AEP are increased and COE is decreased compared to the baseline configuration.

Twist and chord distributions for S2 are shown in Figure 6.4.a and 6.4.b, respectively.

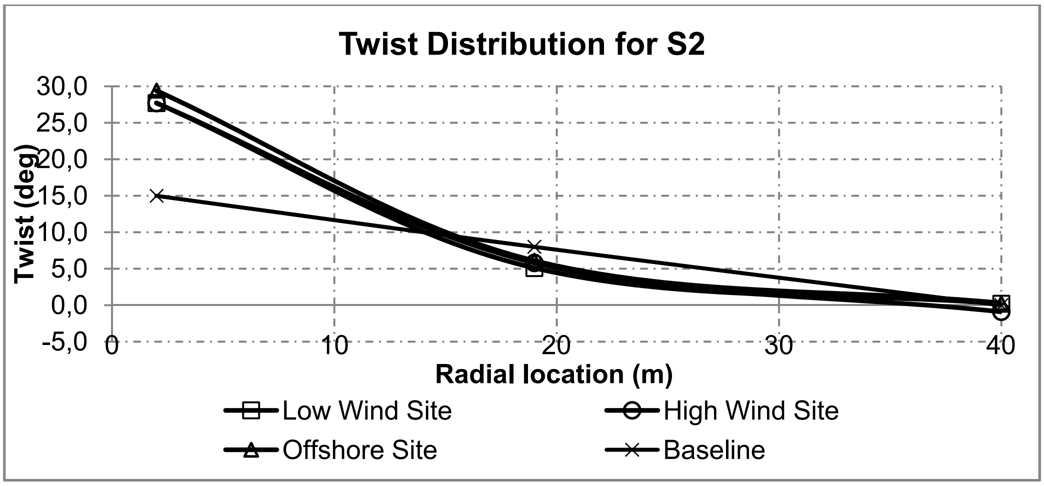

(a)

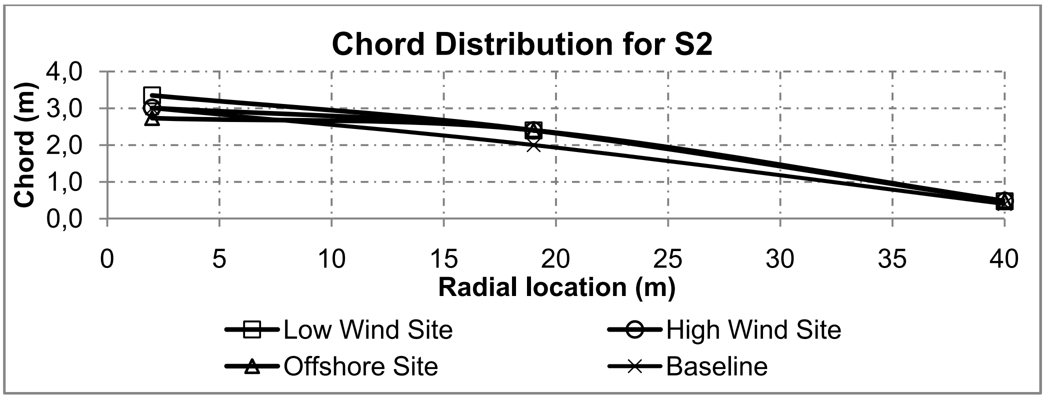

(b)

Figure 6.4 Resultant (a) Twist and (b) Chord distribution for S2

Scenario 3

Design optimization parameters for the S3 are selected as chord and twist values at root, mid and tip of the blade and also the rated power. NREL S-series airfoil family is used for the blade sections. Resultant optimization parameters and performance parameters are presented in Table 6.10 and Table 6.11.

Table 6.10 Resultant Optimization Parameters for S3

	θ_{root} (deg.)	θ_{mid} (deg.)	θ_{tip} (deg.)	c_{root} (m)	c_{mid} (m)	c_{tip} (m)	Rated Power (MW)
Low Wind Site	27.1	4.8	-0.2	2.84	2.4	0.48	1.597
High Wind Site	26.1	4.8	-0.5	2.73	2.4	0.48	1.612
Offshore Site	29.4	4.1	-0.3	2.63	2.4	0.48	1.678

Table 6.11 Design Optimization Results for S3

	AEP (MWh)	COE (cents/kWh)	LCC/LCC_{BL}	AEP/AEP_{BL}	COE/COE_{BL}
Low Wind Site	2852.6	9.36	1.064	1.230	0.8646
High Wind Site	6528.1	5.11	1.059	1.219	0.8690
Offshore Site	8199.4	4.37	1.045	1.228	0.8508

Results present that optimized rated power is less than the baseline configuration for all wind sites. However, AEP/AEP_{BL} and COE/COE_{BL} rates indicate an improvement in AEP and COE compared to baseline configuration. Although the decrease in rated power will result in a decrease in LCC, LCC/LCC_{BL} rates denote that LCC is higher compared to baseline configuration. This result yields that AEP has more dominant effect on LCC compared to rated power.

Resultant twist and chord distributions for S3 are presented in Figure 6.5.a and 6.5.b, respectively. In Figure 6.5.c, variation of the rated power is shown.

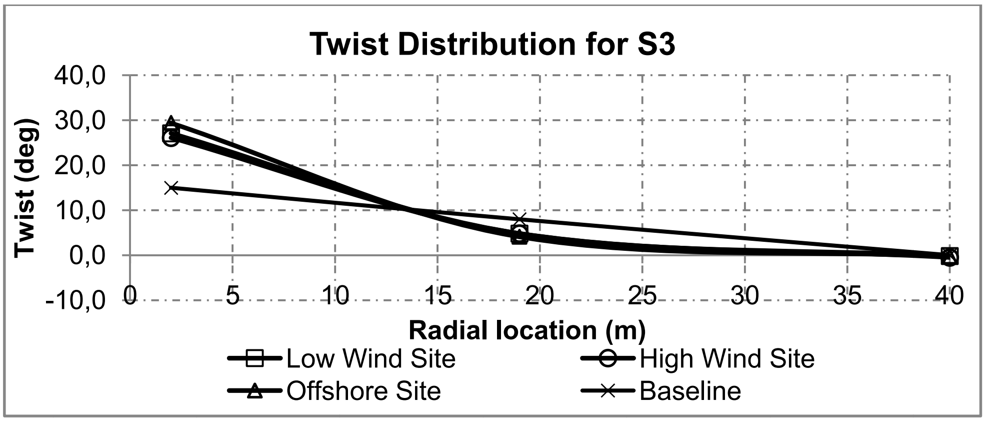

(a)

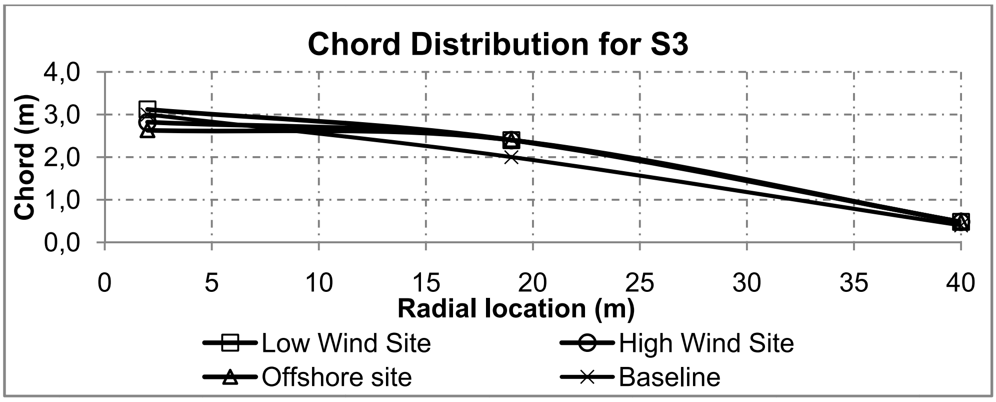

(b)

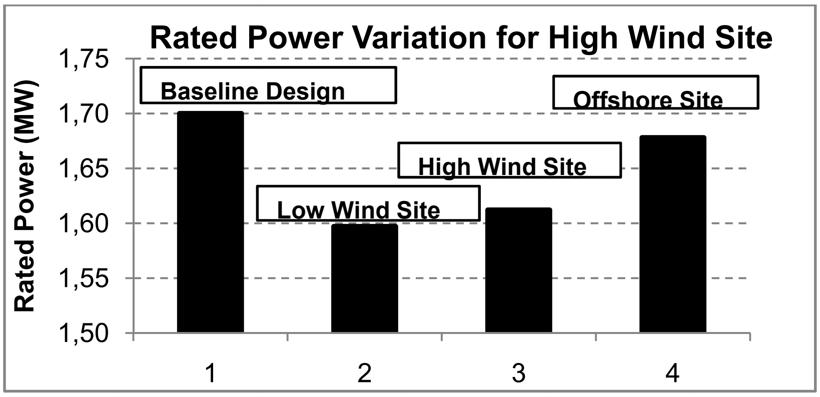

(c)

Figure 6.5 Optimized (a) Twist distribution, (b) Chord distribution and (c) Rated power for S3

6.3.2 Relative Comparison of Different Scenarios

In this section, a relative comparison of optimization results and performance parameters are shown for three selected wind sites: Low Wind Speed, High Wind Speed and Offshore Sites. Moreover, variations of parameters for each scenario are compared.

Low Wind Speed Site

Variations in chord and twist distributions for the three scenarios for the low wind speed site are shown in Figure 6.6.a and 6.6.b respectively.

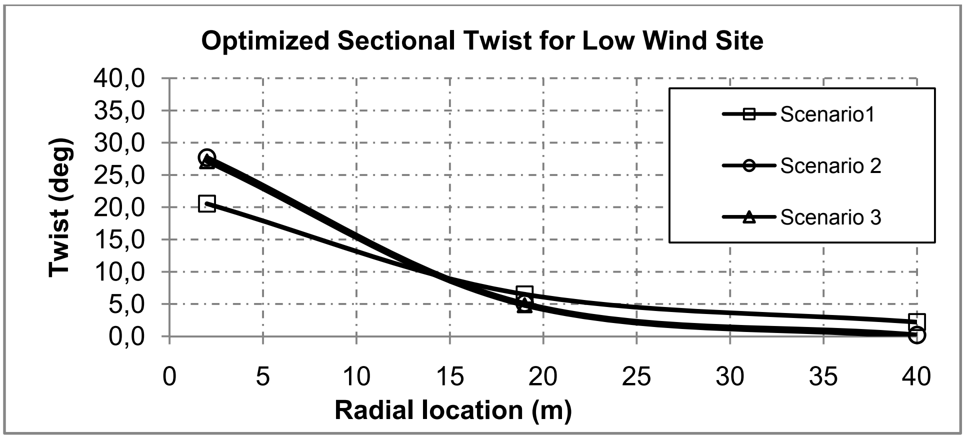

(a)

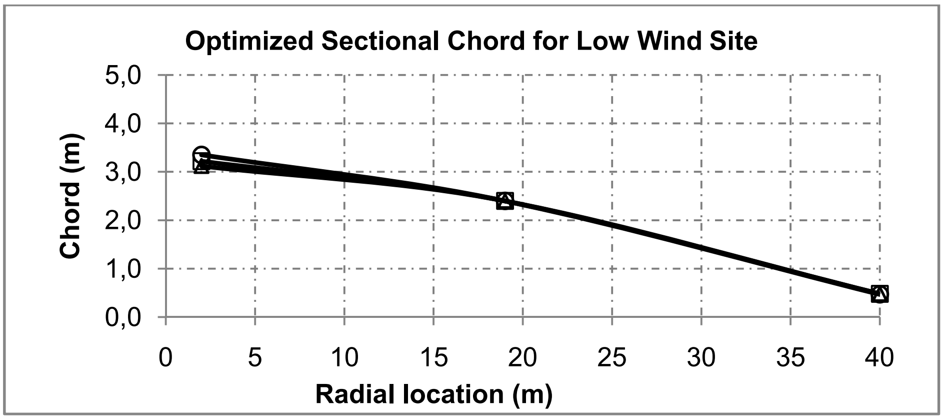

(b)

Figure 6.6 Optimized (a) twist (b) chord for the Low Wind Site for different scenarios.

As seen from Figure 6.6.a, optimum sectional twist distribution of S1 is different than that of S2 and S3. Optimized twist distribution of S2 and S3 are similar, since same airfoil profiles are used for these scenarios. This comparisons show that twist distribution depends on airfoil aerodynamic characteristics as much as on characteristics of wind site characteristics.

Figure 6.7.a and 6.7.b presents the variation of COE and AEP parameters according to Scenario type.

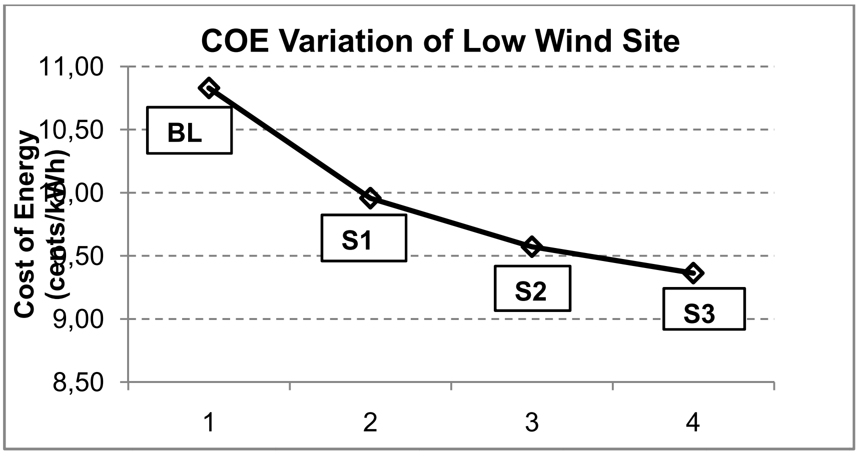

(a)

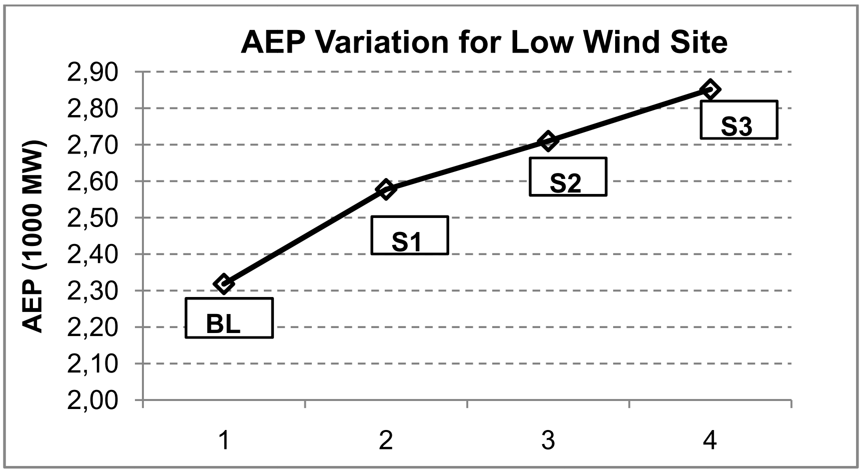

(b)

Figure 6.7 Variations of (a) COE and (b) AEP for Low Wind Site

As seen in Figure 6.7.a and 6.7.b, the designs are improved step by step from baseline to S3. As previously explained, S1 optimizes chord and twist distribution and uses S809 airfoil profile. For S2, NREL S-series airfoil family, which is specifically designed for wind turbines, are used. Therefore, at S2, using specifically designed airfoils increased performance, such as higher AEP and lower COE. Finally, at S3, rated power is used as additional optimization parameter which also resulted in the best performance of all.

High Wind Speed Site

Variations of chord and twist distributions for the high wind speed site according to scenario type are shown in Figure 6.8.a and 6.8.b, respectively.

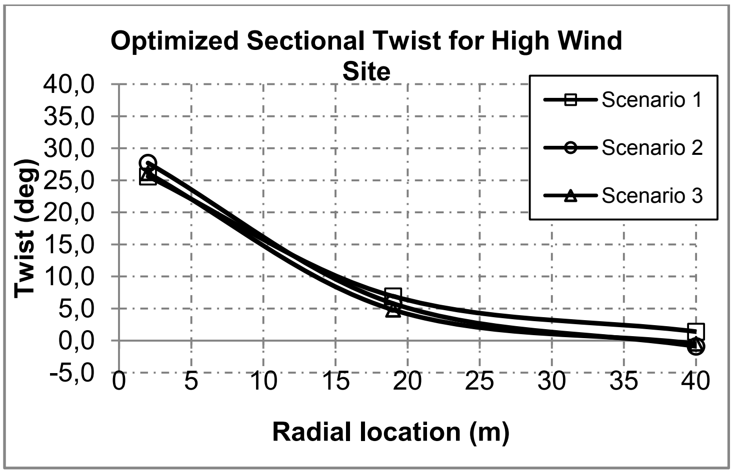

(a)

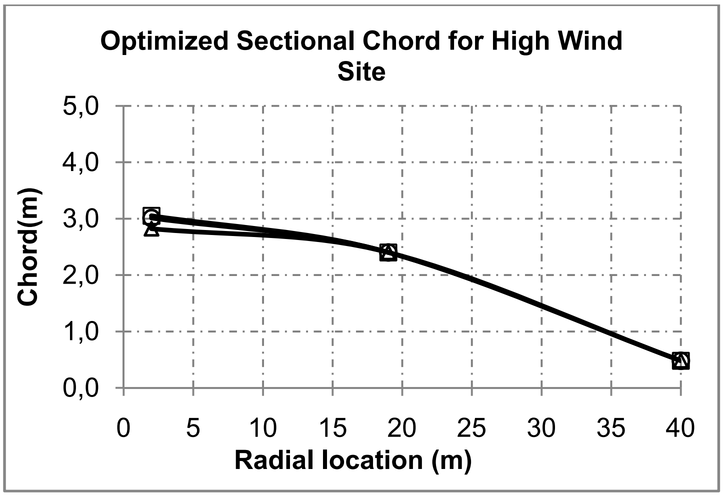

(b)

Figure 6.8 Optimized (a) twist (b) chord for the High Wind Site for different scenarios.

As seen from Figure 6.8.a and Figure 6.8.b, there is a slight difference for optimized twist and chord distributions for different scenarios. However, difference in performance parameters, i.e. COE and AEP are more obvious as shown in Figure 6.9.a and 6.9.b.

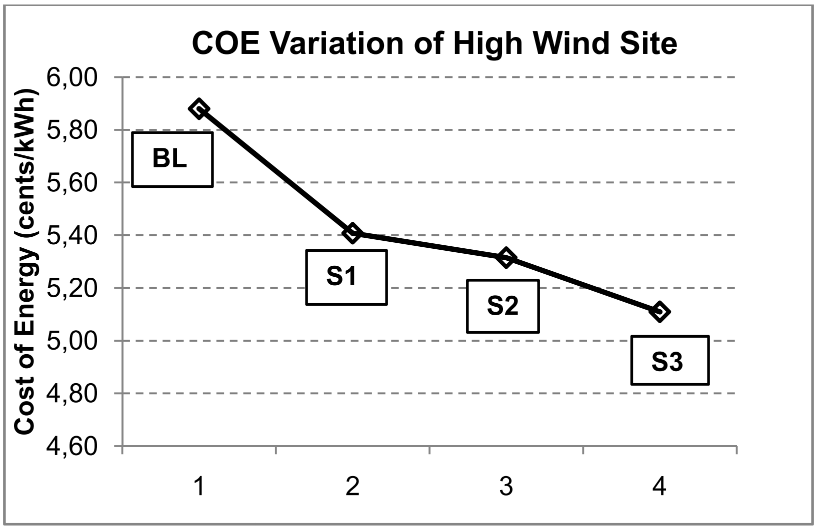

(a)

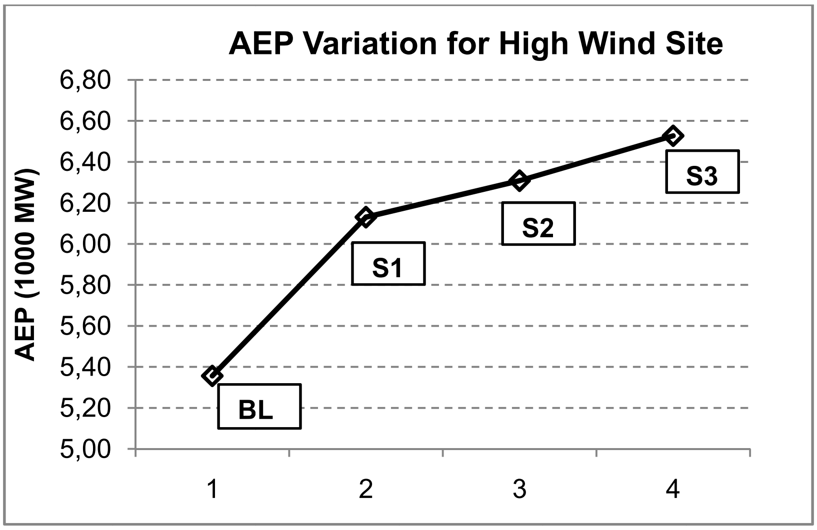

(b)

Figure 6.9 Variations of (a) COE and (b) AEP for High Wind Site

Figure 6.9.a and Figure 6.9.b show that AEP increases and COE decreases from baseline configuration to S3, which means better design is obtained at each step. S3 yields the best performance of all.

Offshore Site:

Variation of chord and twist distributions for offshore site according to scenario type are shown in Figure 6.10.a and 6.10.b respectively.

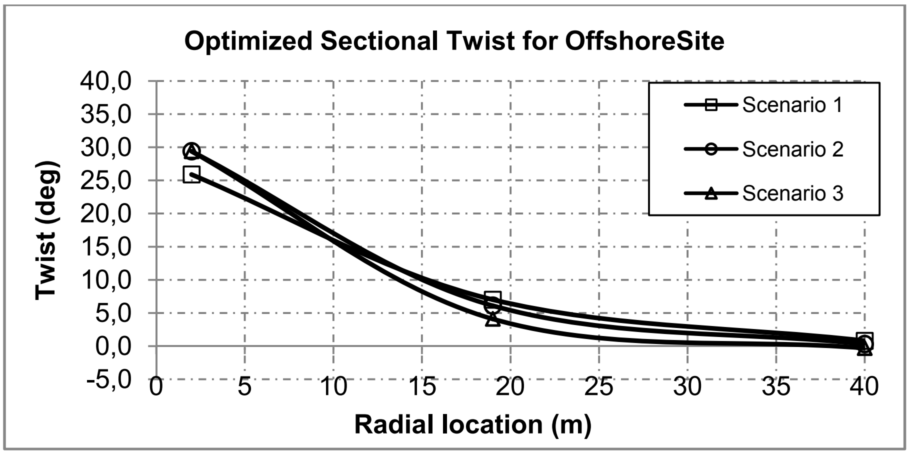

(a)

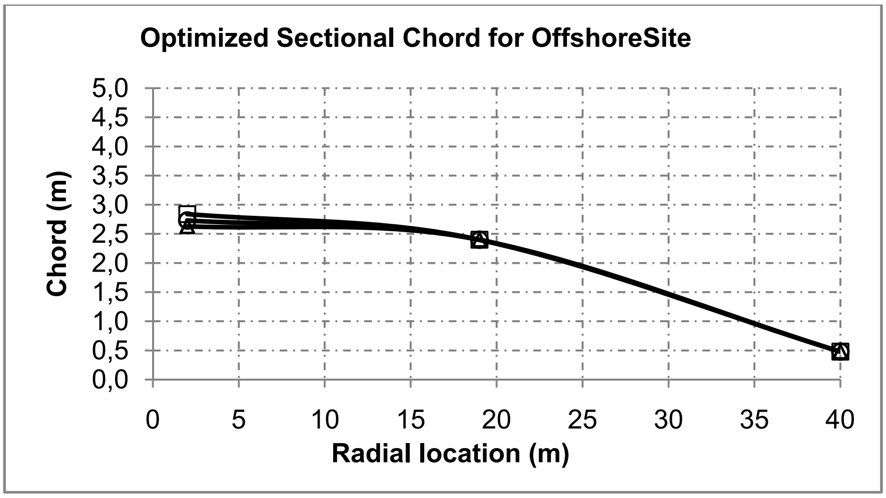

(b)

Figure 6. 10 Optimized (a) twist (b) chord for the Offshore Site for different scenarios.

As seen from Figure 6.10.a, twist distribution show different characteristics for each scenario. However, chord distributions are much alike except the root chord. Variation of performance parameters, COE and AEP, are shown in Figure 6.11.a and 6.11.b, respectively.

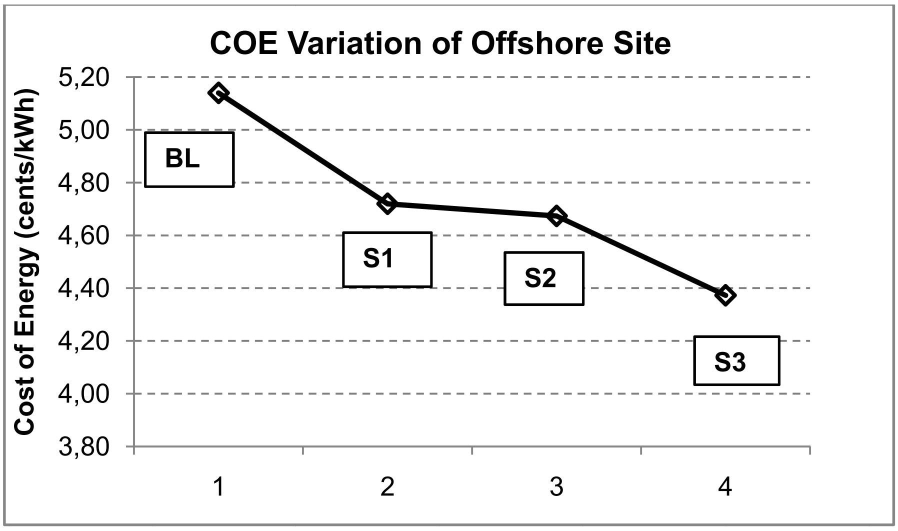

(a)

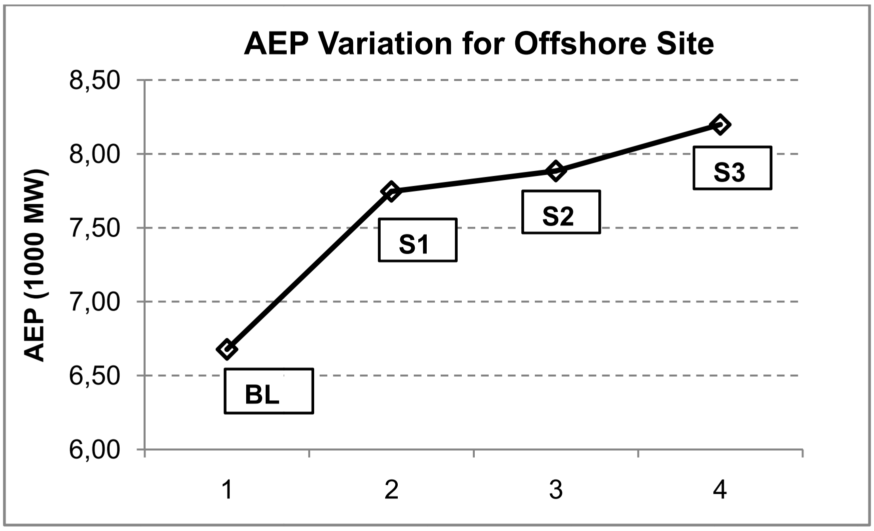

(b)

Figure 6.11 Variations of (a) COE and (b) AEP for Offshore Site

The variation of AEP and COE for offshore site shows similar characteristics as other wind sites. Every step of the design optimization yields better performance compared to previous.

6.3.3 The Effect of Airfoil Profile

S1 and S2 perform the same design optimization; however, different airfoil profiles are used. S1 uses S809 airfoil for all sections, whereas S2 uses NREL S-series airfoil family, which is designed specifically for wind turbines. Two scenarios are compared to show how specifically designed airfoil profiles improve the performance of the wind turbine as shown in Figure 6.12. Improvement designated as decrease in COE and increase in AEP.

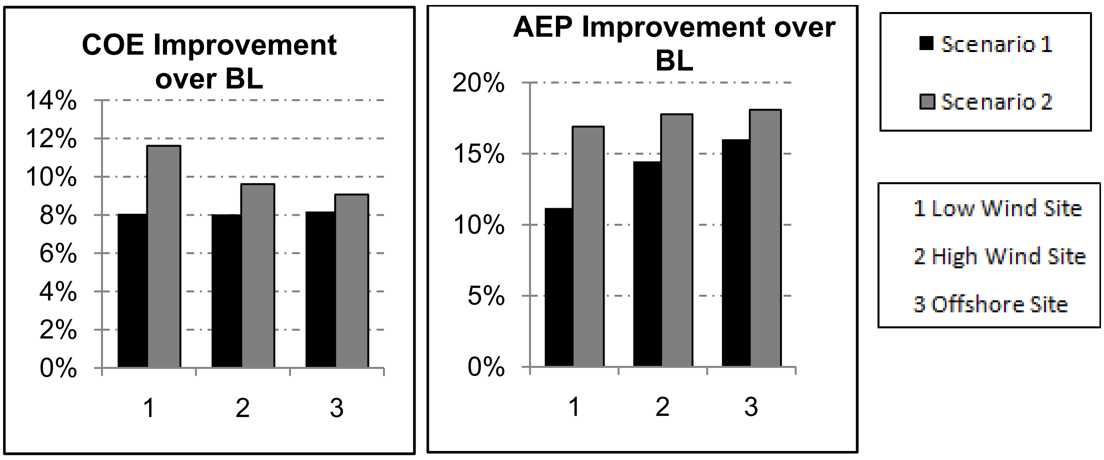

Figure 6.12 COE and AEP Improvement of S1 and S2 compared to baseline design

As seen from Figure 6.12, improvement both on COE and AEP are observed for all wind sites. However, S2 shows better performance improvements of COE and AEP compared to S1. The COE differences between two scenarios are, 3.5% for Low Wind Site, 1.5% for High Wind Site and 1% for Offshore Site. The AEP differences between two scenarios are, 5.5% for the Low Wind Site, 3.3% for the High Wind Site, and 2% for the Offshore Site. This result emphasizes on importance of using different airfoils through blade section.

6.3.4 The Effect of Rated Power

The only difference between S2 and S3 is using the rated power as an additional optimization parameter in S3. Therefore by comparing two scenarios, effect of rated power on COE and AEP can be observed. Comparison of two scenarios in terms of COE and AEP are shown in Figure 6.13.

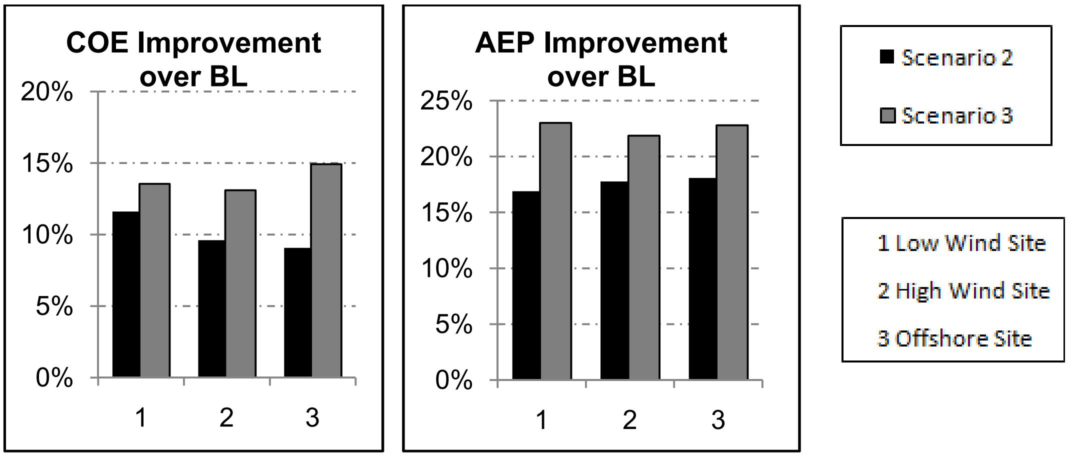

Figure 6.13 COE and AEP Improvement of S2 and S3 compared to baseline design

Since rated power has great impact on cost of wind turbine, hence on COE, compared to other optimization parameters, S3 yields better COE and AEP improvements than S2 for all wind sites, as seen in Figure 6.13. The COE differences between two scenarios are, 2% for Low Wind Site, 3.5% for High Wind Site and 6% for Offshore Site. The AEP differences between two scenarios are, 6% for the Low Wind Site, 4% for the High Wind Site, and 5% for the Offshore Site.

6.3.5 The Effect of Wind Site

Effect of wind sites are shown by comparing the resultant AEP and COE of the optimized wind turbines as shown in Figure 6.14 and Figure 6.15. Due to high wind speed profile the offshore site has the maximum AEP and the minimum

COE for each scenario, whereas Low Wind Site has the minimum AEP and the maximum COE as explained.

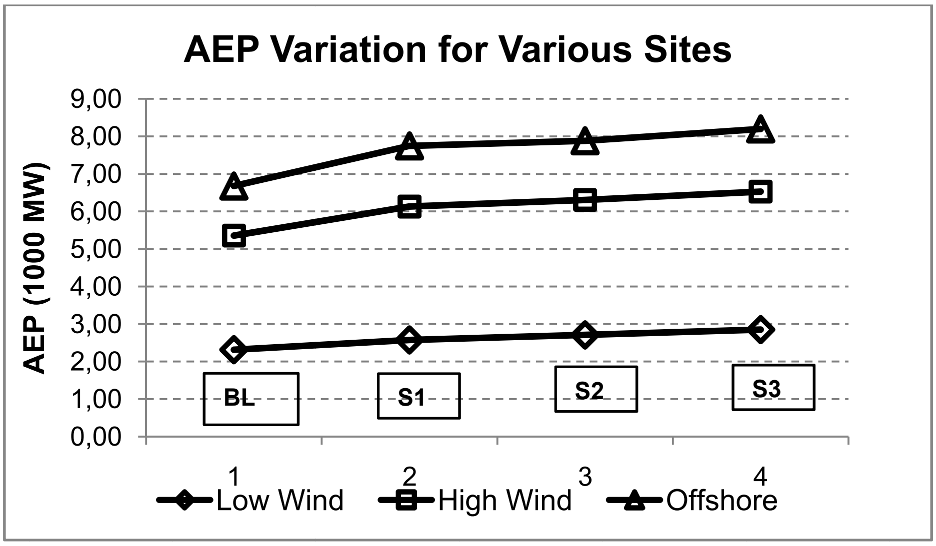

Figure 6.14 The resultant AEP for wind sites selected.

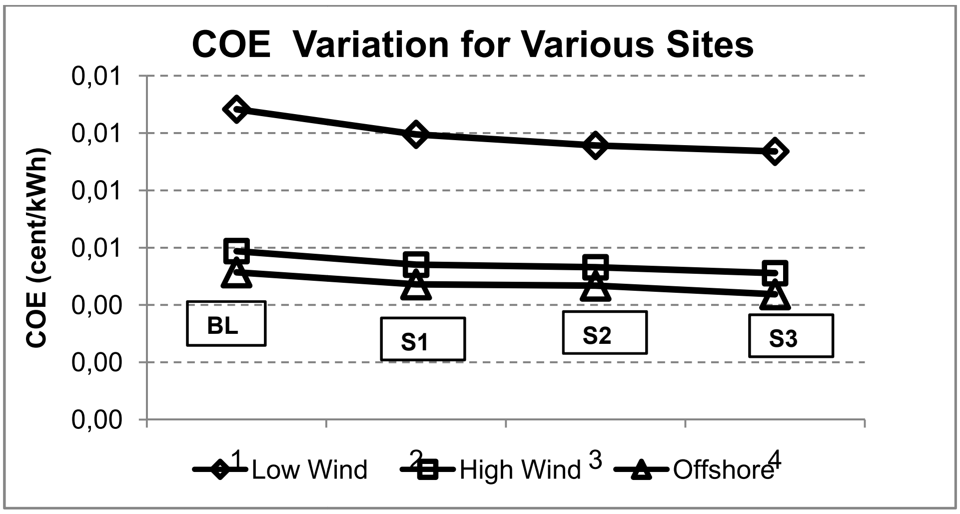

Figure 6.15 The resultant AEP for wind sites selected.

CHAPTER 7

CONCLUSION

In this study a design optimization methodology is generated to obtain a three-bladed Horizontal Axis Wind Turbine (HAWT) that has minimum “Cost of Energy” for a given wind characteristic of a specific site. An in-house code, named **WindCOE**, is developed to perform the design optimization procedure. An open source, Genetic Algorithm based Optimization routine has been coupled to the design code. The design optimization parameters are selected as chord and twist distributions based on three locations (i.e. tip, mid and root) on the blade and as the rated power. The objective function for optimization is the “Cost of Energy”.

Annual Energy Production is modeled by computing the power of wind turbine and the frequency of the wind for each speed from cut-in to cut-out. Power production is obtained using Blade Element Momentum (BEM) theory and Wind frequency is modeled by Weibull distribution.

Annual cost of the wind turbine is modeled using Life Cycle Cost model, which calculates cost of the wind turbine components and operating service.

The airfoil database consists of a constant airfoil profile and airfoil family. The details of the derivation of lift and drag coefficients of these airfoils by numerical methods are presented.

Three scenarios have been generated to investigate the effect of different parameters on Cost of Energy. First and second scenarios try to find the optimum chord and twist distributions for a constant rated power. The first scenario uses a single airfoil profile that does not change through the blade span, and the second scenario uses NREL airfoil family that has a pre-determined airfoil variation across the span. Third scenario includes the rated power also as an optimization parameter along with the others. For each scenario, design optimization is performed for three different wind sites, whose Weibull parameters are known, to evaluate the effect of different wind characteristics on wind turbine performance and COE.

Results of the design optimization show that specifically designed airfoils improve the performance; i.e Cost of Energy is reduced. Moreover, optimizing the rated power as well as other optimization parameters also resulted in reduced Cost of Energy. Performing the design optimization for different sites shows that, the optimum configuration is affected by the wind site characteristics.

Future works that can be helpful to improve the design optimization methodology are:

- Extension of the airfoil database by using already existing airfoils or by designing new airfoils.
- Cost model can be improved so that it includes the effect of geometrical properties such as chord and twist on cost of the wind turbine.
- Atmospheric turbulence model can be added to Blade Element Momentum Analysis in order to investigate the effect of turbulence on energy production.
- Effect of material type on blade components and tower costs can be evaluated.

REFERENCES

[1] *Kyoto Protocol website*., 13 November 2009, Retrieved from http://unfccc.int/kyoto_protocol/items/2830.php

[2] European Wind Energy Assosication, *Wind Energy-The Facts.* 12 March 2009, Retrieved from http://www.ewea.org/fileadmin/ewea_documents/documents/publications/WETF/WETF.pdf

[3] Hau, E.,2005. *Wind Turbines- Fundamentals, Technologies, Application,Economics.2nd edition.* Springer.

[4] Ackermann, T., 2005. *Wind Power in Power Systems.* 1st edition, Wiley .

[5] Fugslang P., Madsen H.A. "Optimization Methods for Wind Turbine Rotors". *Journal of Wind Engineering and Industrial Aerodynamics* , 80(1999) 191-206.

[6] L. Fingersh, M. H.. 2006. *Wind Turbine Design Cost and Scaling Model.* NREL/TP-500-40566, National Renewable Energy Labarotory,USA.

[7] Griffin D. A.. 2000. *NREL Advanced Research Turbine (ART) Aerodynamic Design of ART-2B Rotor Blades.*NREL/SR-500-28473 National Renewable Energy Laboratory,USA

[8] Fuglsang P., Bak C. , Schepers J. G., Bulder B. , Olesen A., Van Rossen R., Cockerill T..2010. *Site Specific Design Optimization of Wind Turbines.* JOR3-CT98-0273,Risø National Laboratory (Risø).

[9] Moriarty J.and Hansen C.J. .2005. *AeroDyn Theory Manual.* National Renewable Energy Laboratory,USA

[10] Schmidt M..2007. *The Economic Optimization of Wind Turbine Design* .,M.Sc Thesis, Georgia Institute of Technology.

[11] Ceyhan, Ö..2008. *Aerodynamic Design and Optimization of Horizontal Axis Wind Turbines by using BEM Theory and Genetic Algorithm.*M.Sc Thesis, Middle East Technical University,Ankara.

[12] Tangler, J.L and Somers, D.M.1995. *NREL Airfoil Families for HAWTs.* ational Renewable Energy Laboratory.

[13] Fuglsang P and Dahl K.S..1998. *Design of the Wind Turbine Airfoil Family RISO-A-XX.* RISO National Laboratory, Roskilde, Denmark.

[14] Caroll D., *Genetic Algorithm Optimization Code by FORTRAN77*. Retrieved 3 February 2009, from http://www.cuaerospace.com/carroll/ga.html

[15] Haupt R. and Haupt S.E.. 2004. *Practical Genetic Algorithms.2nd edition,* Wiley.

[16] *Wind Turbine Warehouse*. Retrieved, 15 November 2009, from http://www.windturbinewarehouse.com/

[17] Leishman, J. G. 2002. *Principles of Helicopter Aerodynamics.* 2nd edition, Cambridge University Press.

[18] Buhl M.. 2005. *A New Empirical Relationship between Thrust Coefficient and Induction Factor for the Turbulent Windmill State.*NREL/TP-500-36834. National Renewable Energy Laboratory.USA.

[19] Manwell J. F., McGowan J.G. and Rogers A.L. 2002. *Wind Energy Explained, Theory, Design and Application.* John Wiley & Sons.

[20] Schepers, J. G., Brand A.J. , Bruining A., Graham J.M.R., Hand M.M., Infield D.G., Madsen H.A., Maeda T., Paynter J.H., van Rooij R., Shimizu Y., Simms D.A., Stefanatos N. 2002. *Final Report of IEA Annex XVIII: Enhanced Field Rotor Aerodynamics Database.* Energy Research Centre of Netherlands.

[21] Anderson J.D. Jr.. 2001. *Fundamentals of Aerodynamics.3rd edition,* McGraw Hill.

[22] Hansen C. , *NWTC Design Codes (AirfoilPrep).* Retrieved 11 January 2009, from http://wind.nrel.gov/designcodes/ preprocessors/airfoilprep/

[23] Çevik, M. (2009). *Design and Optimization of a Mixed Flow Compressor Impeller using Robust Design Methods.* Ankara: Middle East Technical University.

[24] Bilgili M., Şahin B. and Kahraman A.. 2004. Wind Energy Potential in Antakya and İskenderun Regions, Turkey. *Renewable Energy ,Vol 29*, pp 1733–1745.

[25] Eskin N., Artar H. and Tolun S. Wind energy potential of Gökçeada Island in Turkey. *Renewable & Sustainable Energy Reviews , Vol 12* ,pp 839-851.

[26] Neumann T. and Riedel V. FINO 1 Platform: Update of the Offshore Wind Statistics. *DEWI Magazin February 2006 Nr. 28*

APPENDIX A

RESULTS OF AIRFOIL NUMERICAL ANALYSIS

NREL Airfoil Family for blades up to 15m

First airfoil set is shown in Figure A.1 This airfoil family includes S815 Airfoil up to 30 % of the blade, S814 Airfoil between 30- 40 % of the blade, S825 Airfoil between 40-75 % of the blade and S826 Airfoil between 75-100 % of the blade.

Figure A.1 Airfoil distribution of NREL Airfoil family for blades up to 15m.

Reynolds number characteristics of first airfoil set are given in Table A.1. As an engineering assumption, airfoil aerodynamic characteristics does not change with the Reynolds number Therefore only design Reynolds number are considered by numerical analyses.

Table A.1 Design Reynolds Number of NREL Airfoil family for blades up to 15m.

Airfoil	**Reynolds Number**
S815	$1.2 * 10^6$
S814	$1.5 * 10^6$
S825	$2 * 10^6$
S826	$1.5 * 10^6$

S814 Airfoil

Lift and drag coefficients of S814 Airfoil, obtained from numerical analysis are shown in Figure A.2 (a) and (b). Extrapolated aerodynamic coefficients are shown in Figure A.3

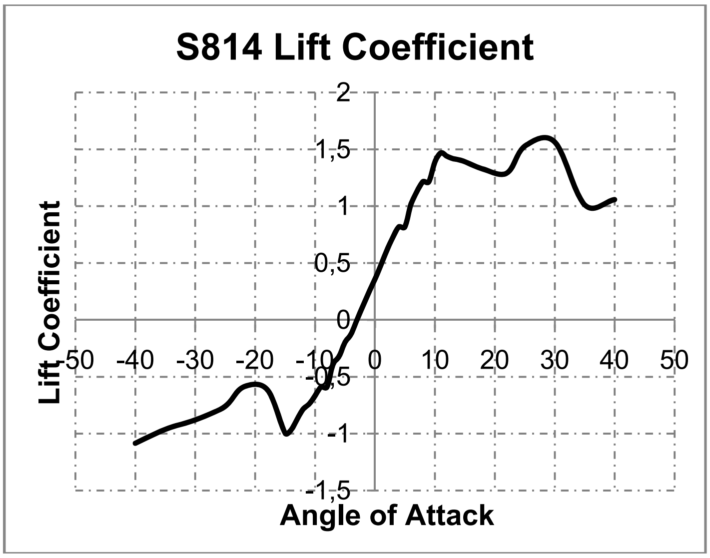

(a)

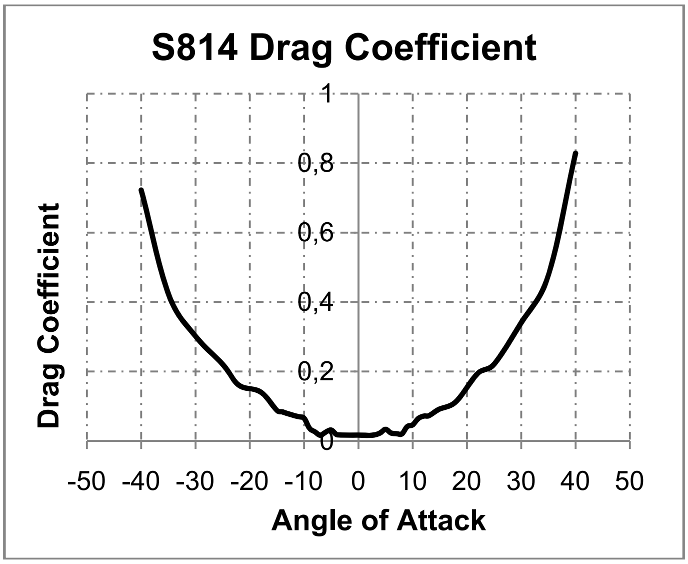

(b)

Figure A.2 (a) Lift Coefficient (b) Drag Coefficient of S814 airfoil obtained from numerical analysis

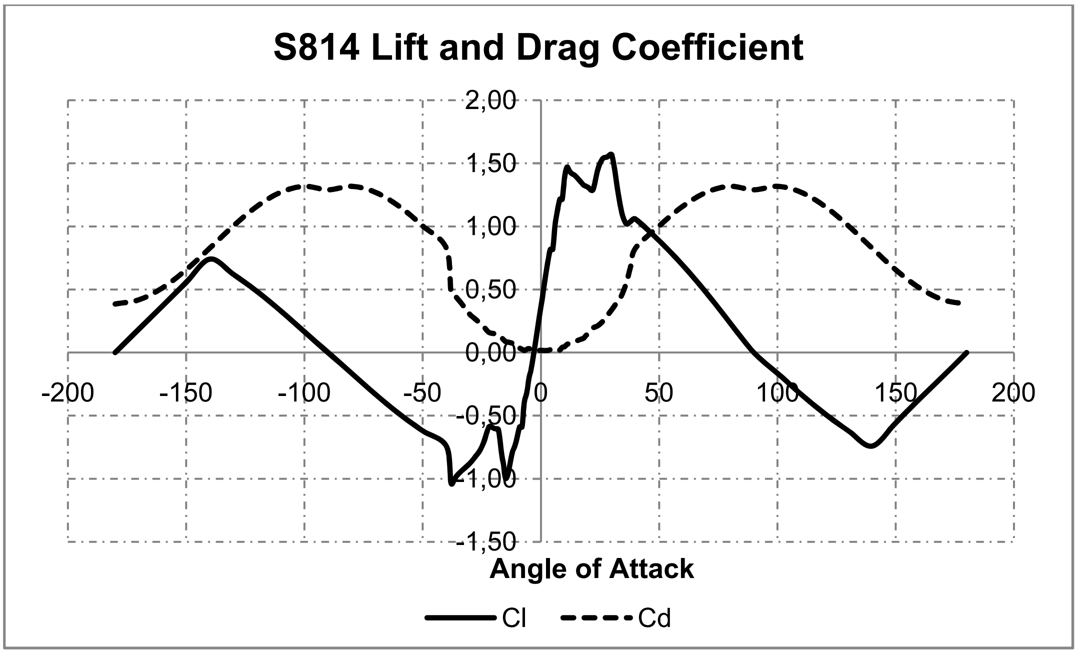

Figure A.3 Airfoil Extrapolated Lift and Drag Coefficients of S814

S815 Airfoil

Lift and drag coefficients of S815 Airfoil, obtained from numerical analysis are shown in Figure A.4 (a) and (b). Extrapolated aerodynamic coefficients are shown in Figure A.5.

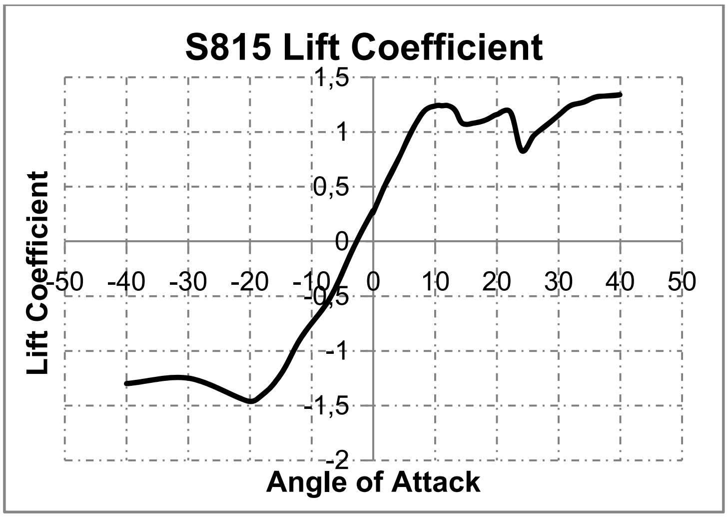

(a)

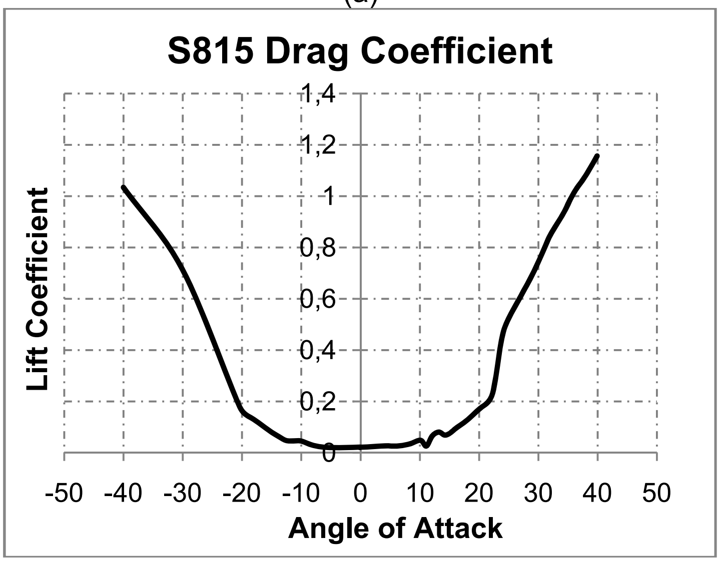

(b)

Figure A. 4 (a) Lift Coefficient (b) Drag Coefficient of S815 airfoil obtained from numerical analysis

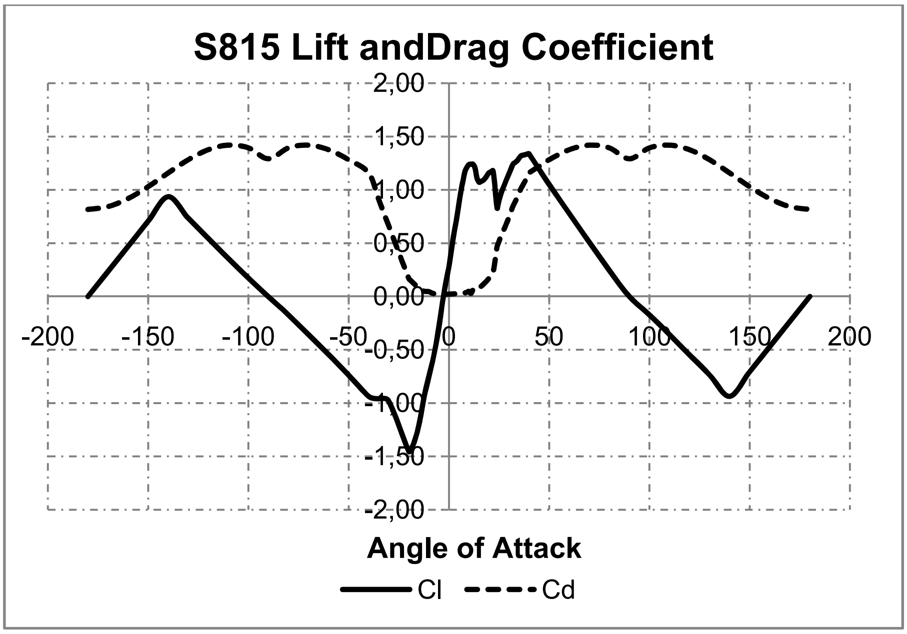

Figure A.5 Airfoil Extrapolated Lift and Drag Coefficients of S815

<u>S825Airofil</u>

Lift and drag coefficients of S825 Airfoil, obtained from numerical analysis are shown in Figure A.6 (a) and (b). Extrapolated aerodynamic coefficients are shown in Figure A.7

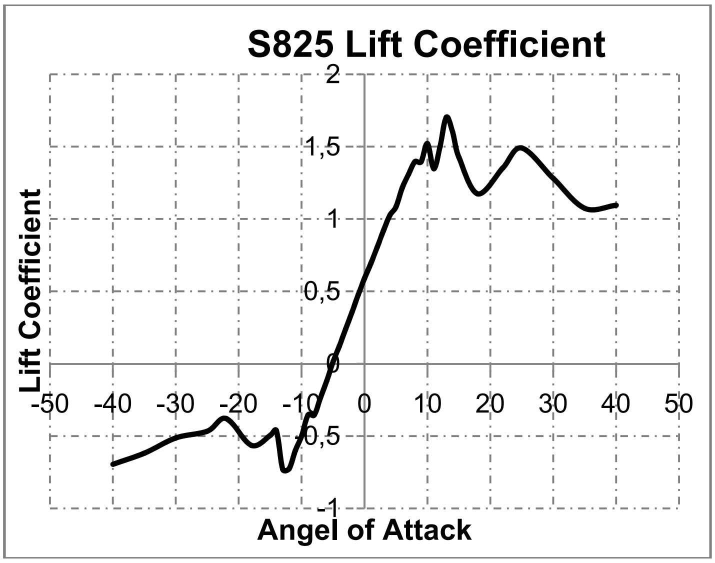

(a)

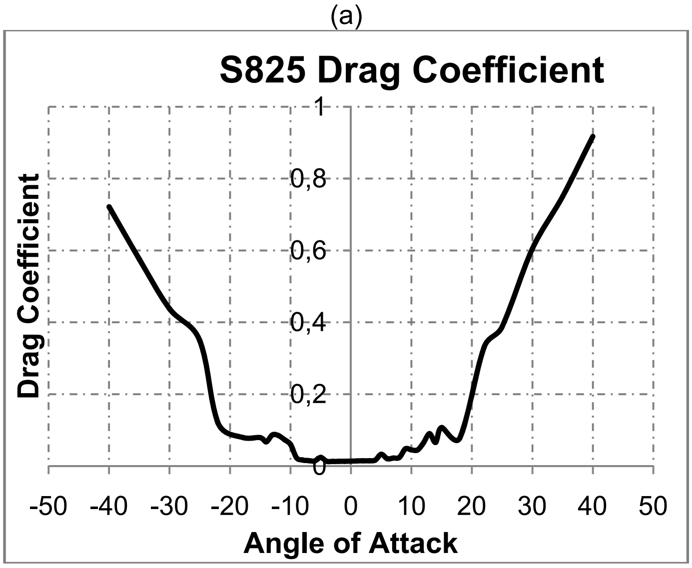

(b)

Figure A.6 (a) Lift Coefficient (b) Drag Coefficient of S825 airfoil obtained from numerical analysis

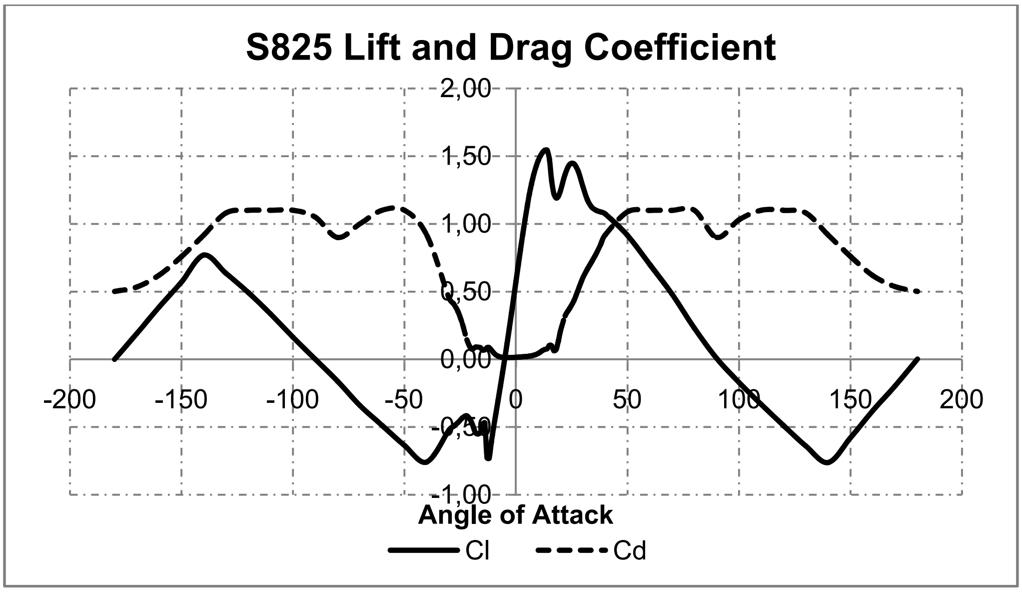

Figure A.7 Extrapolated Lift and Drag Coefficients of S825 Airfoil

<u>S826 Airfoil</u>

Lift and drag coefficients of S826 Airfoil, obtained from numerical analysis are shown in Figure A.8 (a) and (b). Extrapolated aerodynamic coefficients are shown in Figure A.9.

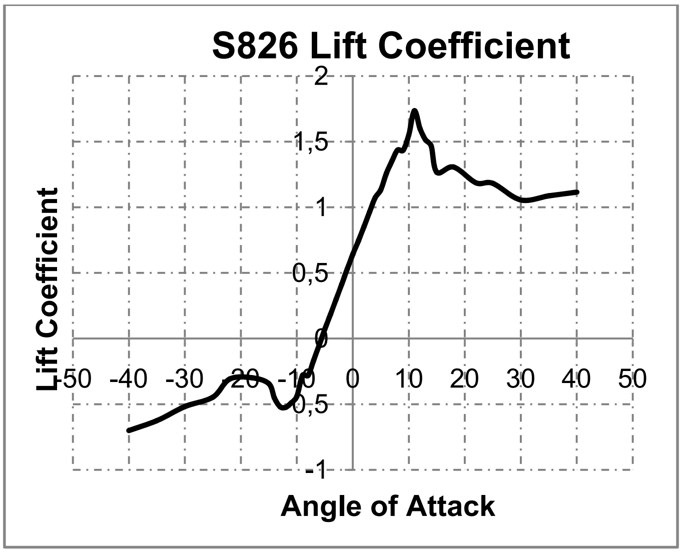

(a)

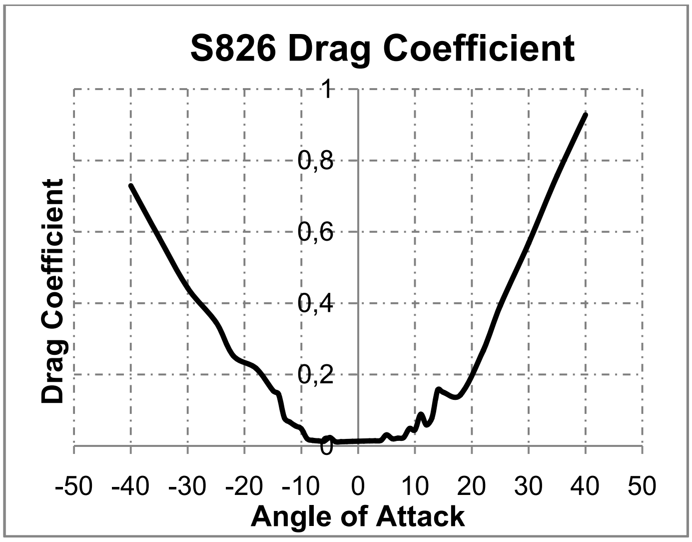

(b)

Figure A.8 (a) Lift Coefficient (b) Drag Coefficient of S826 airfoil obtained from numerical analysis

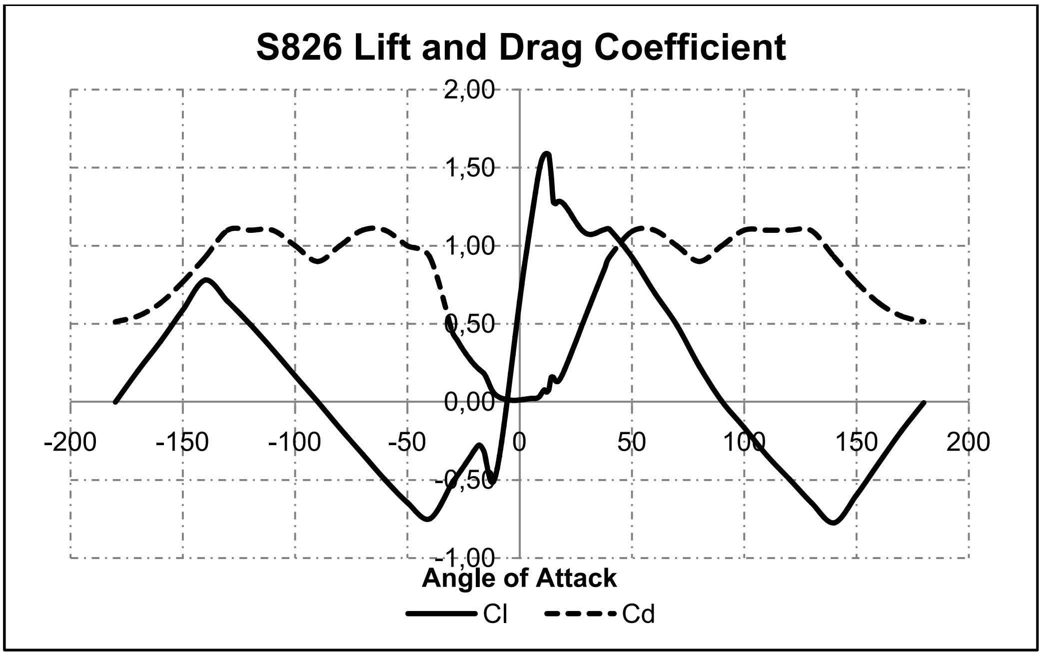

Figure A.9 Extrapolated Lift and Drag Coefficients of S826 Airfoil

NREL Airfoil Family for blades greater than 15m

Second set of airfoils are shown in Figure A.10. This airfoil family includes S818 Airfoil up to 40 % of the blade, S816 Airfoil between 40-75 % of the blade and S817 Airfoil between 75-100 % of the blade. As an engineering assumption, airfoil aerodynamic characteristics does not change with the Reynolds number Therefore only design Reynolds number are considered by numerical analyses. Reynolds number characteristics of first airfoil set are given in Table A.2.

Figure A.10 Airfoil distribution of NREL Airfoil family for blades longer than 15m.

Table A.2 Design Reynolds numbers of NREL Airfoil family for blades longer than 15m.

Airfoil	**Reynolds Number**
S818	$2.5*10^{6}$
S816	$4*10^{6}$
S817	$3*10^{6}$

S816 Airfoil

Lift and drag coefficients of S816 Airfoil, obtained from numerical analysis are shown in Figure A.11. Extrapolated aerodynamic coefficients are shown in Figure A.12.

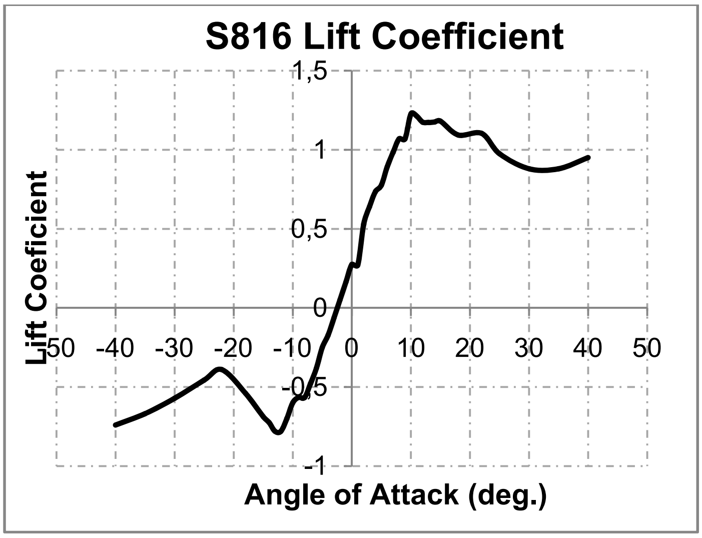

(a)

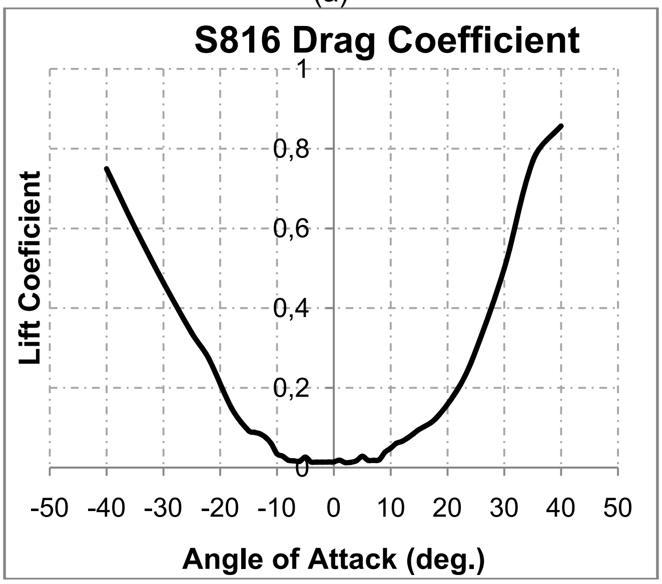

(b)

Figure A. 11 (a) Lift Coefficient (b) Drag Coefficient of S816 airfoil obtained from numerical analysis

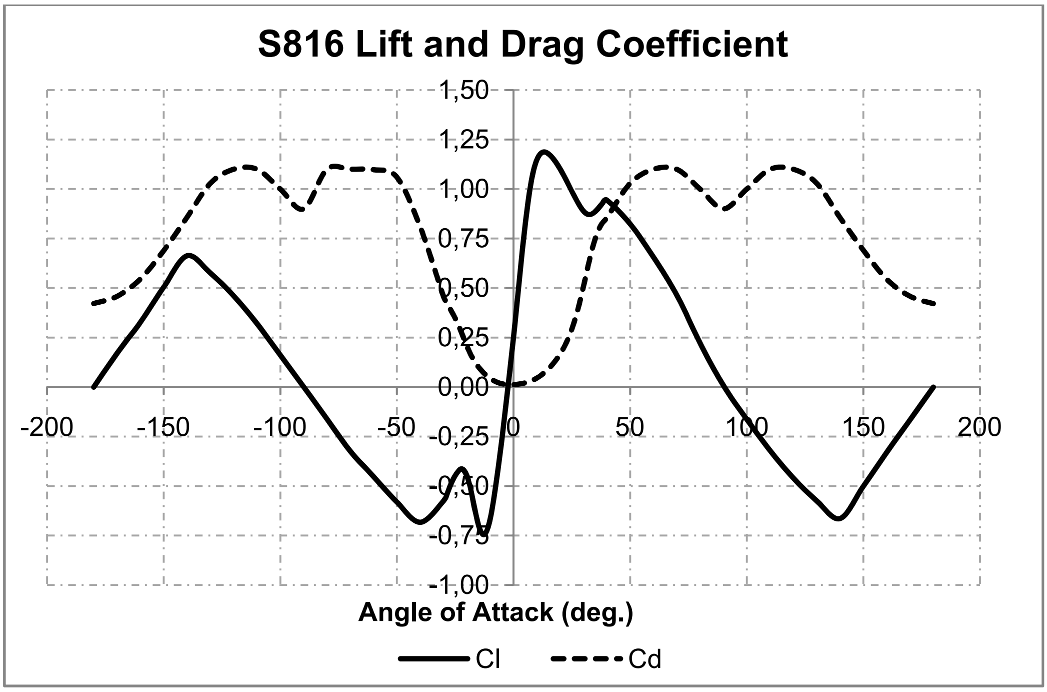

Figure A.12 Extrapolated Lift and Drag Coefficients of S816 Airfoil

S817 Airfoil

Lift and drag coefficients of S817 Airfoil, obtained from numerical analysis are shown in Figure A.13 (a) and (b). Extrapolated aerodynamic coefficients are shown in Figure A.14.

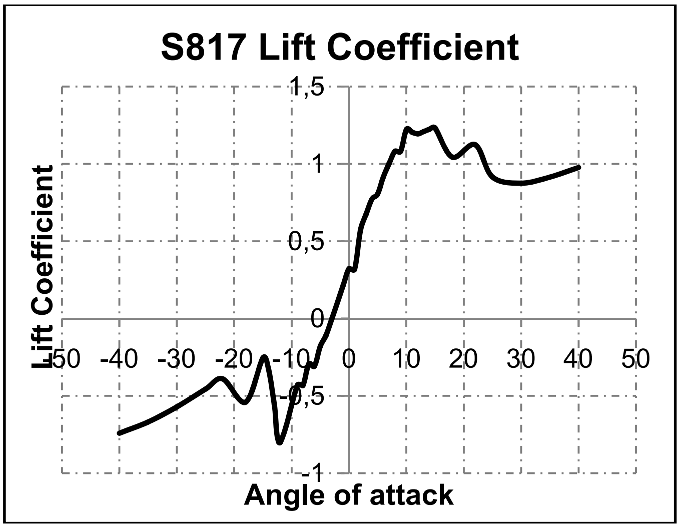

(a)

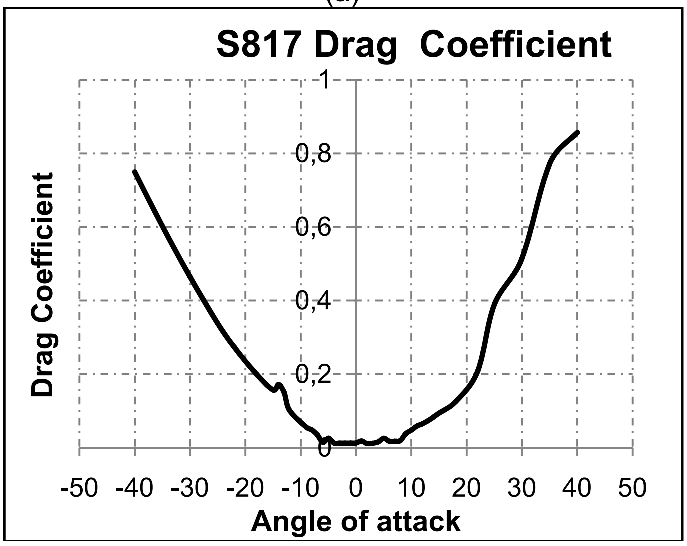

(b)

Figure A. 13 (a) Lift Coefficient (b) Drag Coefficient of S817 airfoil obtained from numerical analysis

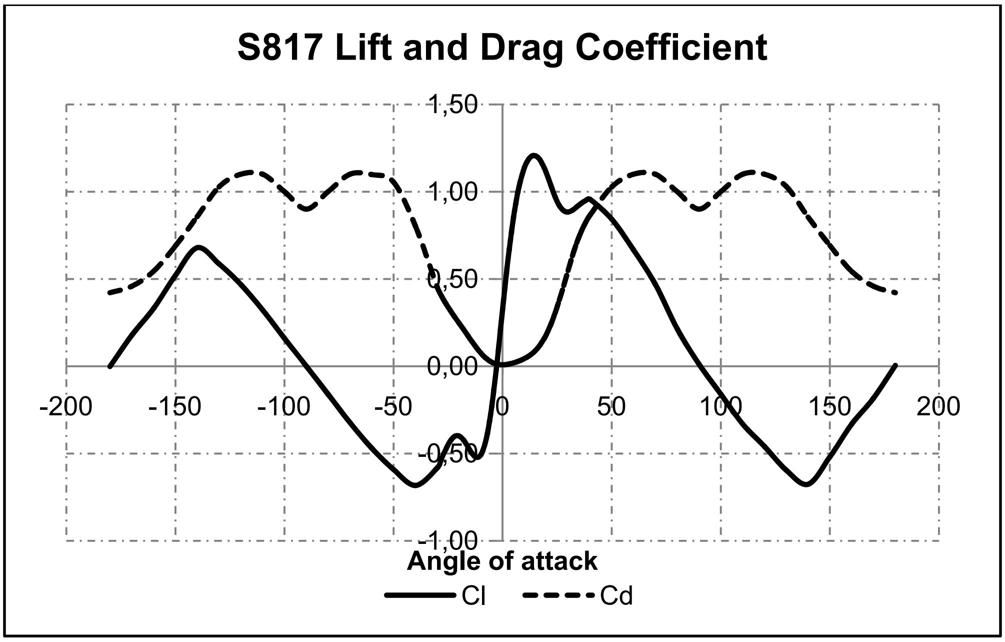

Figure A. 14 Extrapolated Lift and Drag Coefficients of S817 Airfoil

S818 Airfoil

Lift and drag coefficients of S818 Airfoil, obtained from numerical analysis are shown in Figure A.15 (a) and (b). Extrapolated aerodynamic coefficients are shown in Figure A.15.

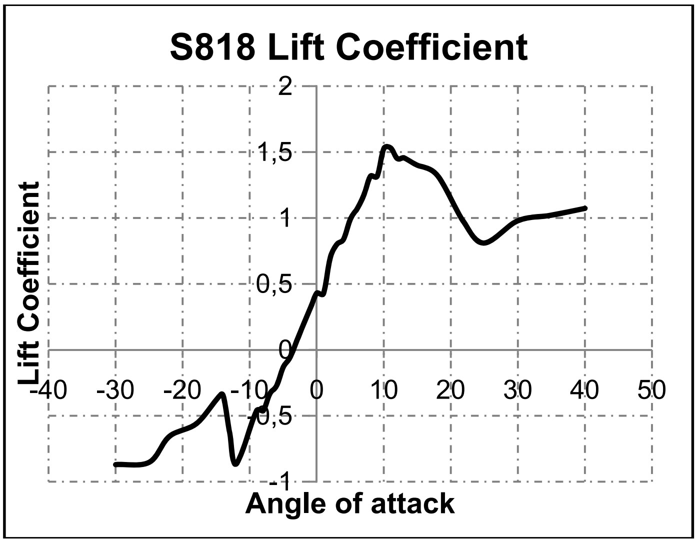

(a)

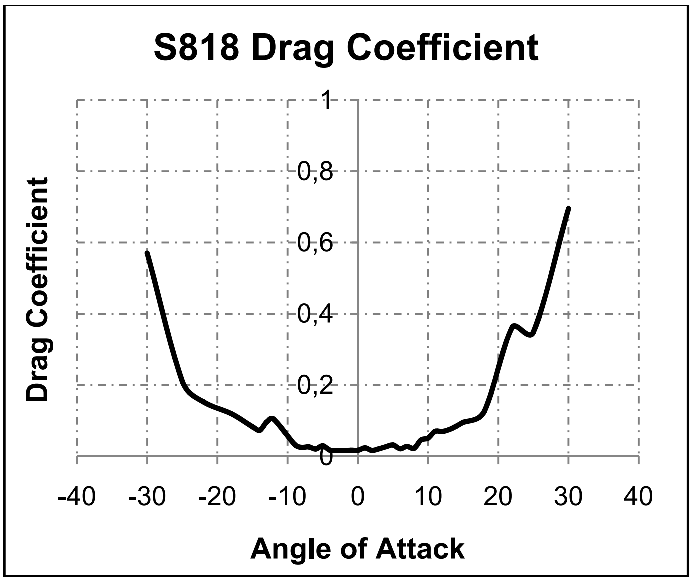

(b)

Figure A.15 (a) Lift Coefficient (b) Drag Coefficient of S818 airfoil obtained from numerical analysis

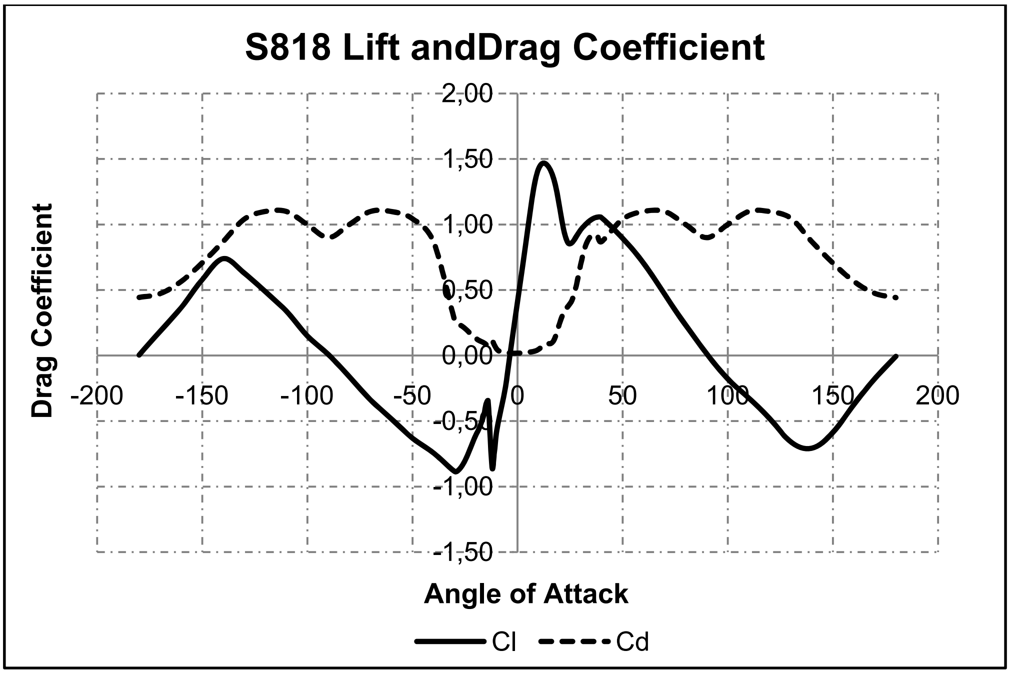

Figure A.16 Extrapolated Lift and Drag Coefficients of S818 Airfoil